PDOL-Based Solid Electrolyte Toward Practical Application: Opportunities and Challenges

Hua Yang[1], Maoxiang Jing[1] ✉, Li Wang[2] ✉, Hong Xu[2], Xiaohong Yan[1], Xiangming He[2] ✉

## HIGHLIGHTS

- The poly(1,3-dioxolane) (PDOL) electrolyte demonstrates promising potential for practical application due to its advantages in in-situ polymerization process, high ionic conductivity, and long cycle life.

- This review focuses on the polymerization mechanism, composite innovation, and application of PDOL electrolytes.

- This review provides a comprehensive summary of the challenges associated with the PDOL electrolyte and makes forward-looking recommendations.

ABSTRACT Polymer solid-state lithium batteries (SSLB) are regarded as a promising energy storage technology to meet growing demand due to their high energy density and safety. Ion conductivity, interface stability and battery assembly process are still the main challenges to hurdle the commercialization of SSLB. As the main component of SSLB, poly(1,3-dioxolane) (PDOL)-based solid polymer electrolytes polymerized in-situ are becoming a promising candidate solid electrolyte, for their high ion conductivity at room temperature, good battery electrochemical performances, and simple assembly process. This review analyzes opportunities and challenges of PDOL electrolytes toward practical application for polymer SSLB. The focuses include exploring the polymerization mechanism of DOL, the performance of PDOL composite electrolytes, and the application of PDOL. Furthermore, we provide a perspective on future research directions that need to be emphasized for commercialization of PDOL-based electrolytes in SSLB. The exploration of these schemes facilitates a comprehensive and profound understanding of PDOL-based polymer electrolyte and provides new research ideas to boost them toward practical application in solid-state batteries.
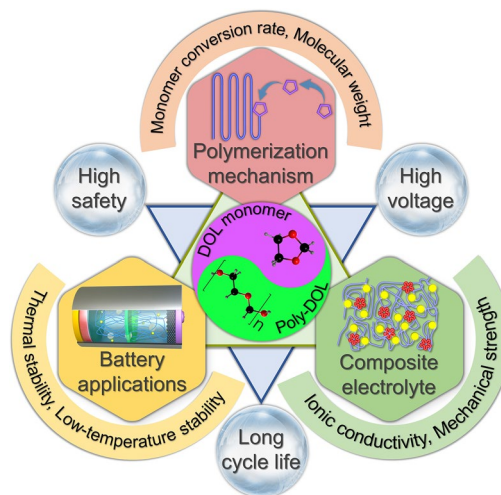
✉ Maoxiang Jing, mxjing2004@ujs.edu.cn; Li Wang, wang-l@tsinghua.edu.cn; Xiangming He, hexm@tsinghua.edu.cn
1 Institute for Advanced Materials, School of Materials Science and Engineering, Jiangsu University, Zhenjiang 212013, People's Republic of China
2 Institute of Nuclear and New Energy Technology, Tsinghua University, Beijing 100084, People's Republic of China

1 Introduction

The mass production of lithium-ion batteries (LIB) has profoundly transformed our daily lives over the past few decades, with continuous performance improvement and widespread use [1]. In recent years, the development of electric vehicles has driven the demand for key performance indicators of lithium-ion batteries, including energy density, safety, and service life [2], to a new height. Solid-state lithium batteries (SSLB) employ a solid-state ion conductor to replace conventional liquid electrolytes. With the advantages of less flammable electrolytes and more stable electrochemical properties, they are considered one of the most competitive solutions to break through the performance bottleneck of traditional liquid lithium-ion batteries in the future [3]. The core solid electrolyte (SE) of SSLB has been continuously optimized and developed into two major categories: solid polymer electrolytes (SPE) and solid inorganic electrolytes

(SIE). SPE has promising application prospects due to its lower cost, superior interface contact, and ease of production and processing [3–6]. SPE currently comprises solid electrolyte systems that mainly consist of materials such as polyethylene oxide (PEO) [7–11], polyvinylidene fluoride (PVDF) [12–18], pyrolytic polyacrylonitrile (PAN) [19–21], and poly(vinylidene fluoride-co-hexafluoropropylene) (PVDF-HFP) [22–24], poly(methyl methacrylate) (PMMA) [23–29], poly(vinyl chloride) (PVC) [30], which have relatively good electrochemical performance owing to their respective advantages. PEO is one of the earliest and most extensively investigated SPEs, exhibiting numerous advantages such as cost-effectiveness, excellent thermal stability, and remarkable flexibility. However, it suffers from challenges related to low ionic conductivity and environmentally detrimental preparation processes. Therefore, SPEs encounter research bottlenecks due to limitations such as narrow electrochemical stability window, low room temperature ionic
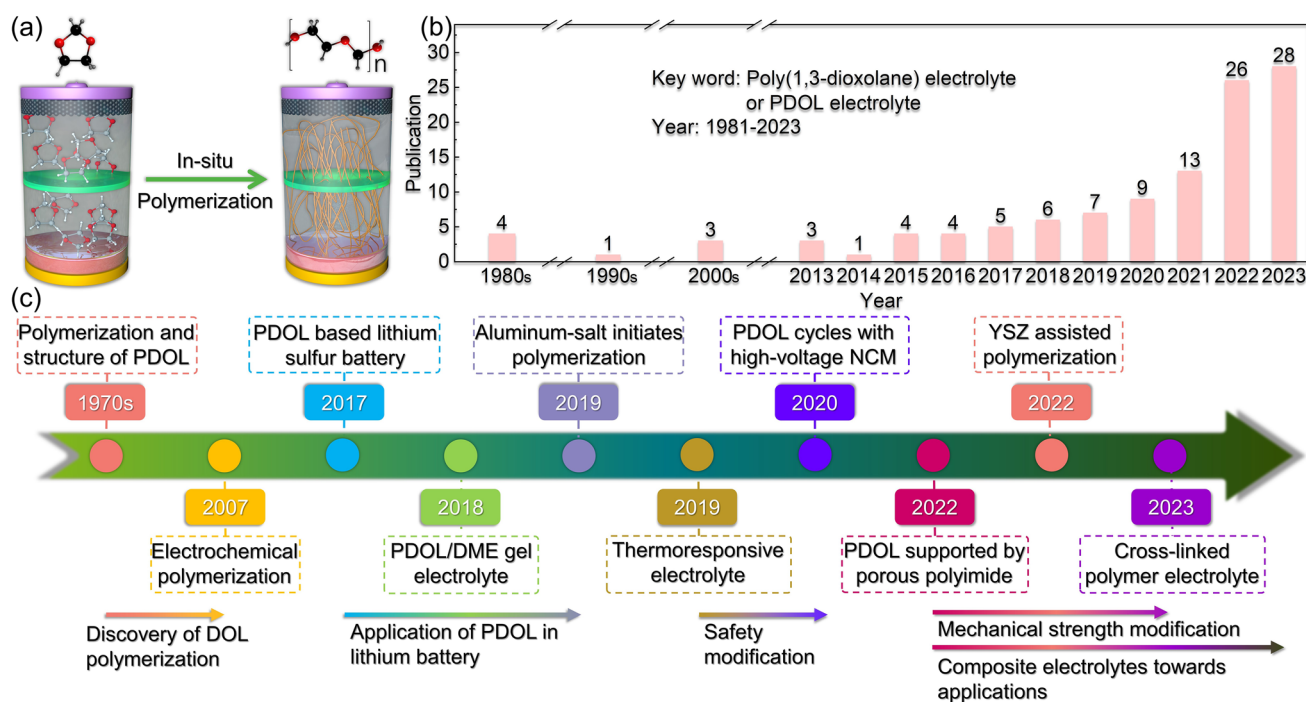

Fig. 1 Overview of research progress on PDOL polymer. **a** Schematic diagram of in-situ polymerization of DOL monomer inside the battery. **b** Number of publications related to PDOL electrolyte in each year (Keyword: Poly(1,3-dioxolane) electrolyte or PDOL electrolyte; Data from Web of Science). **c** Development process of PDOL polymer: The polymerization of DOL and the structure of PDOL began to be studied (1968–1972) [60–62], Current is used to initiate DOL polymerization (2007) [63], PDOL inhibits the shuttle effect of polysulfides in lithium-sulfur batteries (2017) [56], PDOL/DME gel electrolyte enabled stable cycle with LiFePO$_4$ cathode (2018) [58], Initiating DOL polymerization with anhydrous participation of trace aluminum salts (2019) [64], PDOL/PLAS thermoresponsive electrolyte prevents thermal runaway (2019) [65], Realizing normal cycling of PDOL initiated with the assistance of AlF$_3$ and high-voltage NCM cathode (2020) [66], Porous polyimide supported PDOL enhances the mechanical strength of the electrolyte (2022) [67], PDOL added by YSZ enables long life cycling at high voltage (2022) [68], PDOL-based cross-linked electrolyte enhances the stability of lithium metal (2023) [69]

conductivity, poor infiltration into porous electrodes, and other defects. SIE has attracted significant attention due to its higher room temperature ionic conductivity, wider electrochemical stability window, higher mechanical strength, and excellent non-flammability. Research on SIE is centered around two main categories: oxides ($Li_7La_3Zr_2O_{12}$, $Li_{1.3}Al_{0.3}Ti_{1.7}(PO_4)_3$, $Li_6BaLa_2Ta_2O_{12}$, etc.) [31–33] and sulfides ($Li_{3.25}Ge_{0.25}P_{0.75}S_4$, $Li_{3.4}Si_{0.4}P_{0.6}S_4$, etc.) [34, 35]. SIE with no leakage and high safety is an ideal electrolyte material for achieving truly solid-state lithium-ion batteries. However, the practical application of SIE poses more apparent challenges. SIE with higher stiffness introduces more interface problem. Its more complex structure results in higher raw material costs, production costs, and more stringent requirements for preparation environment. These limitations have slowed down the development of SSLB, especially in response to the increasing demand for higher electrochemical performance from LIB in terminal products [36–38].

In recent years, in-situ polymerization has emerged as a promising method for the preparation of SE, offering significant advantages in terms of processing and cost [12, 39–46]. Even though in-situ polymerization has the potential for problems such as non-uniform polymerization and unpredictable polymerization rates. This approach involves the conversion of liquid monomers into solid polymers under specific conditions, which effectively addresses the issue of poor interface contact between solid-state electrolytes and solid-state electrodes (Fig. 1a) [38, 39, 47, 48]. Out of these, poly(1,3-dioxolane) (PDOL), which is a polymerization product of 1,3-dioxolane (DOL), shows promising potential for application in lithium-ion batteries. This is attributed to its excellent stability to lithium metal, good antioxidant stability, and facile polymerization method [49].

The remarkable stability of PDOL in relation to lithium metal renders it a suitable candidate for deployment as an artificial solid electrolyte interphase (SEI) and has been extensively studied [50, 51]. Additionally, as an SEI, PDOL can guide the uniform deposition of Li^+ ions and reduce interfacial side reactions [52]. Especially in lithium-sulfur batteries, protecting the lithium metal anode is one of the core strategies to enhance its performance [53–56], the in-situ solidified PDOL can effectively suppress the shuttling of polysulfides and extend their cycling life [57–59].

Although there is limited research on PDOL as an electrolyte, the number of related publications is increasing rapidly recently (Fig. 1b) (based on the Web of Science database), particularly in high-voltage lithium battery systems moving toward practical applications. Given the significant potential application prospects of PDOL polymer electrolytes, this paper provides a categorization and summary of the current research progress of PDOL polymer electrolytes that are still in the early stage of development (Fig. 1c). The paper also summarizes the effects of various modification approaches on polymer properties, and provides a comprehensive understanding of the PDOL polymer electrolyte system for new researchers. Finally, the paper offers reasonable perspectives for future research on the practical application of PDOL in high-voltage lithium batteries.

2 Fundamental Mechanism of DOL Polymerization

Research on the polymerization of DOL can be traced back to 1967 when P. H. Plesch and P. H. Westermann [70] successfully polymerized DOL in dichloromethane using anhydrous perchloric acid as a catalyst. The resulting polymer comprised alternating "formaldehyde" and "epoxyethane" units. Yuya Yamashi [60] found that water decreases the rate of DOL polymerization when catalyzed by triethylammonium boron tetrafluoride. The study also introduced the novel concept that the induction period preceding polymerization is inversely proportional to the initial catalyst concentration. Moreover, the study revealed a linear correlation between the degree of polymerization and conversion, suggesting that the polymerization reaction proceeds even in the absence of water. This study offers a valuable reference for comprehending the internal polymerization dynamics of in-situ polymerization reactions. Furthermore, the copolymerization of DOL and the crystal structure of PDOL were subsequently investigated, providing further theoretical insight into the polymerization of DOL [61, 62].

Subsequently, Aurbach Doron [71] employed a range of techniques such as surface-sensitive Fourier transform infrared spectroscopy (FT-IR), scanning electron microscopy (SEM), X-ray microanalysis, linear sweep voltammetry (LSV), and other methods to investigate the polymerization mechanism of DOL. It was found that electrochemical treatment and contact with Al_2O_3 or $LiAsF_6$ can form $O(-CH_2CH_2-O-CH_2-)_xO$-type polyether substances, which leads to the growth of PDOL chains. This study also
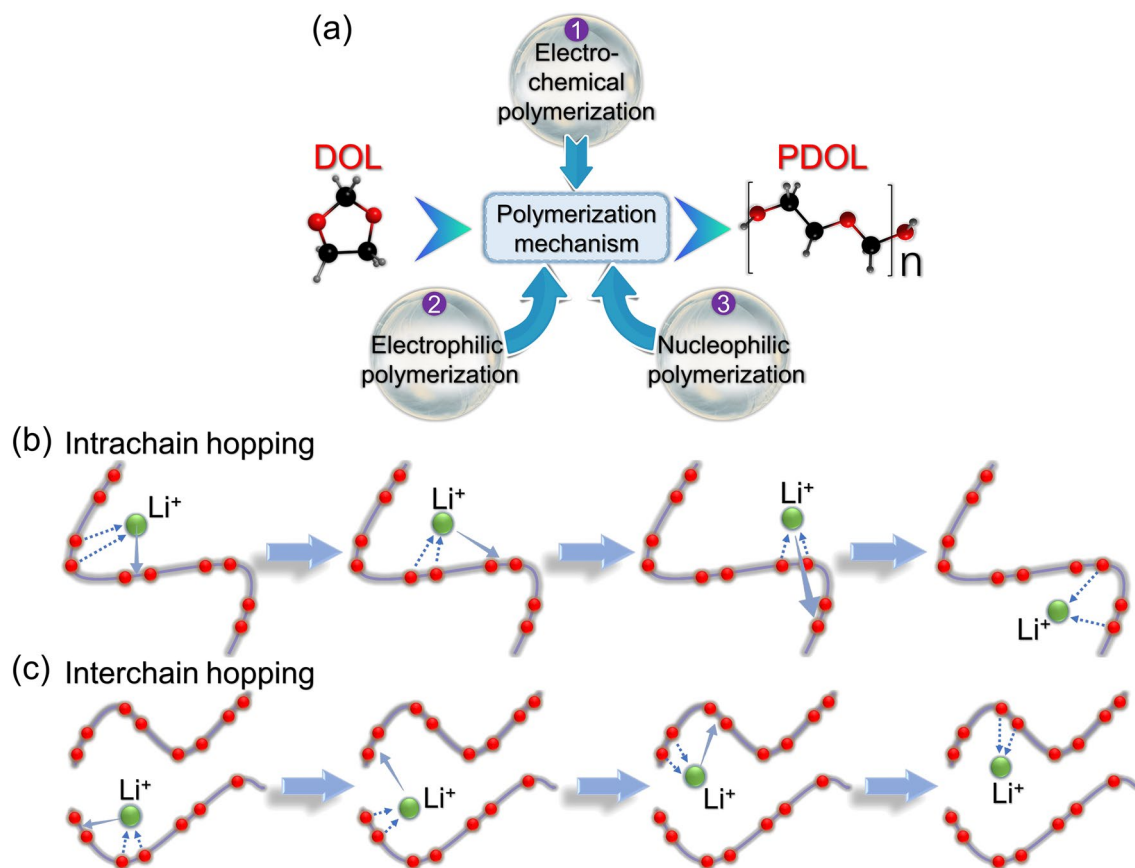
Fig. 2 Polymerization mechanism and Li$^+$ conduction mechanism of DOL. **a** Three polymerization mechanisms of DOL: electrochemical polymerization, electrophilic polymerization, and nucleophilic polymerization [71]. Schematic diagram of **b** intrachain conduction mechanism and **c** interchain conduction mechanism for Li.$^+$ in PDOL [72]

provided comprehensive insight into the polymerization mechanism of DOL, encompassing electrochemical polymerization, electrophilic polymerization, and nucleophilic polymerization (Fig. 2a). These findings offer valuable guidance for selecting initiators for in situ polymerization of DOL in future investigations.

The function of polar atoms in facilitating Li$^+$ conduction in polymers highlights the significance of their content in the polymer chain. The PDOL polymer chain contains a high proportion of polar oxygen atoms, amounting to 43.2 wt%, which is considerably higher than that of PEO (36.4 wt%). This represents a key factor contributing to the generally higher ionic conductivity of PDOL compared to PEO at room temperature.

The ion conductivity of solid polymer electrolytes is typically facilitated by the complexation and decomplexation of Li$^+$ ions with polar atoms [72]. As with PEO segments, the plausible modes of Li$^+$ conduction in PDOL encompass

intrachain conduction (Fig. 2b) and interchain conduction (Fig. 2c). In short-range conduction, Li$^+$ continuously complexes and decomplexes with oxygen atoms on the same PDOL chain under the action of an electric field to achieve migration, that is, intrachain conduction (Fig. 2c). Long-range conduction necessitates interchain conduction, wherein Li$^+$ ions decomplex from an oxygen atom on one PDOL chain under the influence of an electric field and migrate to another chain to complex with its oxygen atom, thereby completing interchain conduction (Fig. 2d).

2.1 Electrochemical Polymerization of DOL

Despite the long-standing use of DOL monomers as electrolyte solvents for lithium-ion batteries, they are highly susceptible to decomposition and consequent battery failure at high voltage [73]. Therefore, early DOL-based solvents were often only used in low-voltage battery systems, such
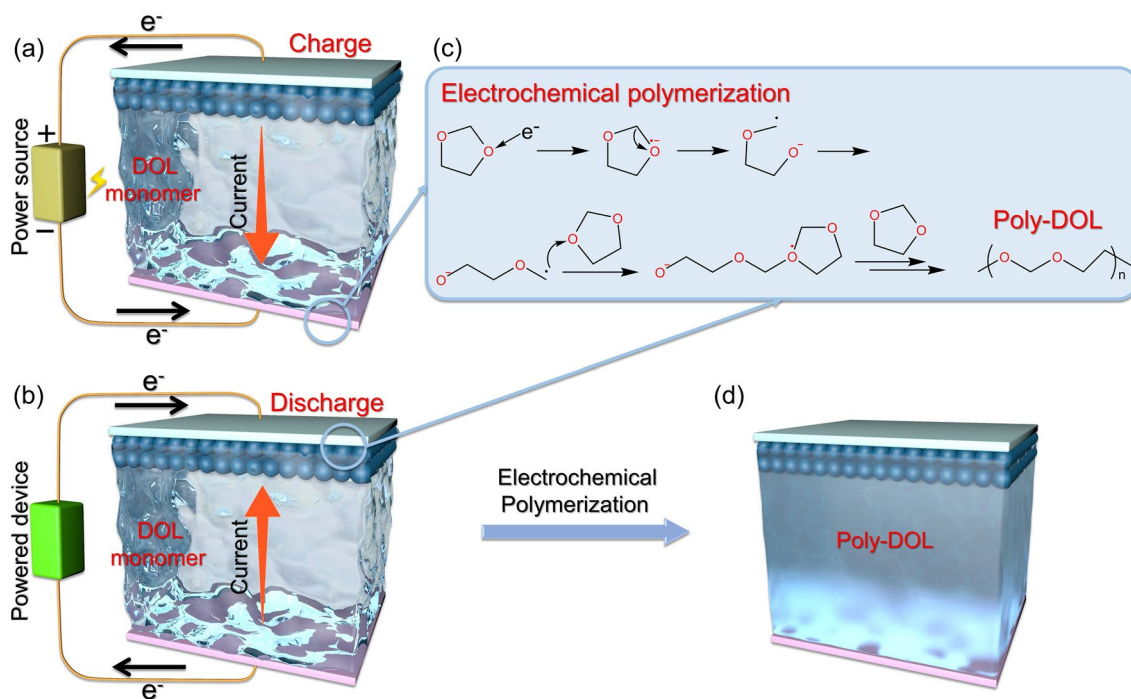
Fig. 3 Applications of current-initiated DOL polymerization. Schematic diagram of electronic and current movements during **a** charging and **b** discharging processes. **c** Electrochemical polymerization mechanism of DOL. **d** Battery state after current-initiated DOL polymerization [45]

as lithium-sulfur batteries. In contrast, as the polymerization product of DOL, PDOL exhibits a markedly improved tolerance to high voltages. Hui Zhan [63] applied an appropriate voltage to in-situ polymerize DOL, resulting in a specific current value that enabled the utilization of DOL-based electrolytes in high voltage LiCoO₂ cathode batteries (Fig. 3a, b). This is a typical example of DOL polymerization caused by electrochemical polymerization. When the oxygen atom on the DOL ring is attacked by electrons, the C-O bond is broken. The oxygen atom at the end of the broken chain

segment is negatively charged and generates -CH₂ radical. And free radicals will combine with the oxygen of DOL monomers to initiate the next polymerization reaction (Fig. 3c). The authors employed an electrolyte comprising 1M LiTFSI in DOL/DME (1,2-dimethoxyethane) at a weight ratio of 2:1 and assembled cells with LiCoO₂ and lithium metal. The cells were subsequently cycled at current densities of 20, 50, 100, 200, and 500 mA g^{-1}. The results indicated that DOL remained inactive and the cycling performance rapidly deteriorated at low current densities
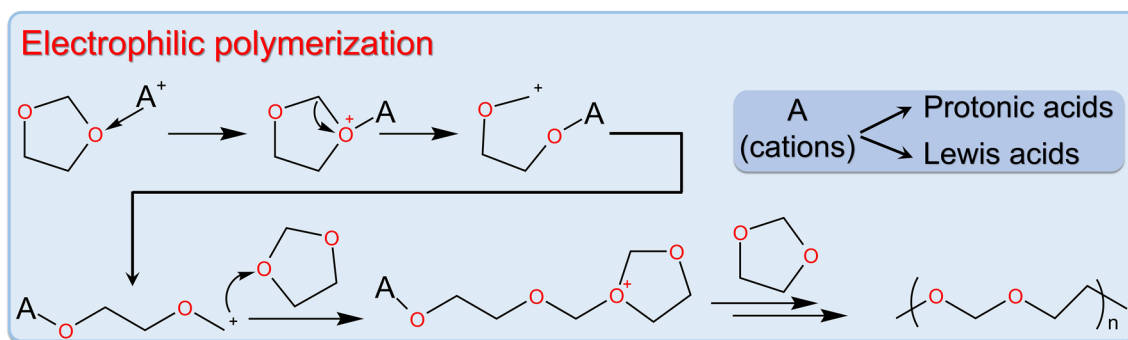

Fig. 4 Electrophilic polymerization mechanism of DOL [71]

Table 1 Classification of different initiators and performance comparison of the PDOL electrolyte initiated by them

Type of initiator	Initiator	Initiation factor	Initiator content	DOL conversion rate (%)	PDOL molecular weight	Electrolyte state	Ionic conductivity (mS cm^{-1})	Oxidation potential (V)	Refs
Lithium salt	LiPF$_6$	Protonic acid	2.0 M	91	~53 000 (Mn)	Gel	3.8	4.6	[58]
	LiPF$_6$	Protonic acid	1.0 wt%	98.5	23 588 (Mw)	Solid	0.28	5.2	[68]
	LiDFOB	Protonic acid	0.3 M	90	/	Gel	0.39	5.1	[75]
	LiBF$_4$	Protonic acid	0.2 M	81.2	–	Solid	0.3	4.9	[76]
	LiFSI	Protonic acid	3.5 M	75	–	Gel	7.9	4.7	[77]
Aluminum salt	Al(OTf)$_3$	Lewis acid	0.5 mM	86	15 000 (Mn)	Solid	1.1	5.0	[64]
	Al(OTf)$_3$ + AlF$_3$	Lewis acid	0.5 mM + 0.3 M	12	18 000 (Mw)	Solid	1.8	4.7	[66]
	AlI$_3$	Lewis acid	600 ppm	84	–	Gel	–	–	[57]
Tin salt	Sn(OTf)$_2$	Lewis acid	2.0 mM	90	12 417 (Mw)	Gel	6.2×10^{-2}	4.9	[78]
	SnF$_2$	Lewis acid	1.5 wt%	92	29 552 (Mw)	Solid	1.7×10^{-2}	5.0	[79]
Other salts	ZnCl$_2$	Lewis acid	25 wt%	–	51 798 (Mn)	–	–	–	[50]
	Sc(OTf)$_3$	Lewis acid	1.0 mM	84	48 963 (Mn)	Solid	8.7×10^{-2}	~5.0	[80]
	Mg(OTf)$_2$	Lewis acid	1.0 wt%	79.9	~57 000 (Mn)	Solid	0.5	4.3	[81]
Acidized materials	Acidized Al$_2$O$_3$	Protonic acid	4.0 wt%	89.6	32 000 (Mn)	Gel	3.37	4.5	[82]
	Acidized CNT paper	Protonic acid	–	–	–	Gel	–	–	[56]
Organic materials	TB	Protonic acid	3.0 wt%	89	–	Solid	1.16	4.8	[83]
	S(C$_2$H$_4$O$_4$)	Lewis acid	0.3 M	88.2	5 391 (Mn)	Solid	0.38	4.7	[84]
	HFiP	Nucleophilic	0.5 wt%	67	–	Gel	1.6	4.7	[85]

(20, 50 mA g^{-1}), whereas the cell exhibited sustained stable cycling over 100 mA g^{-1}. The cyclic voltammetry (CV) curve of the cell corroborated that the polymerization process was irreversible and did not influence the electrochemical performance of LiCoO$_2$. The author believes that these surprising performance improvements are due to current-initiated DOL polymerization forming PDOL (Fig. 3d). The prolonged cycle life demonstrated that the DOL polymerization induced by high current possesses higher dependability in high-voltage battery systems.

2.2 Electrophilic Polymerization of DOL

DOL polymerization often involves the loss or donation of electrons by the oxygen atom on the ring. Consequently, the electrophilic species are ideal initiators for DOL polymerization, and these electrophilic catalytic reactions can quickly and effectively promote the ring-opening polymerization of DOL. These electrophilic catalysts belong to a category of DOL ring-opening initiators, typically in the form of cations,

including protonic acids and Lewis acids [71, 74]. They all initiate ring-opening polymerization by capturing electrons from the oxygen atoms on the DOL ring (Fig. 4).

We have systematically categorized the initiators mentioned in the current literatures, which primarily include lithium salts, aluminum salts, tin salts, other salts, acidified materials, and organic materials (Table 1). Lithium salt initiators often react with trace amounts of water to generate protonic acids for initiating DOL polymerization, while acidified materials rely on the presence of H$^+$ on the surface of the material to initiate polymerization. Metal salts such as aluminum and zinc salts typically exhibit Lewis acidity exhibited by metal cations, leading to DOL ring opening polymerization. Moreover, initiators have a significant impact on the physicochemical and electrochemical properties of the electrolyte, including the DOL conversion rate, PDOL molecular weight, electrolyte state, ion conductivity, and oxidation potential. Therefore, an in-depth exploration of the role of initiators is essential for developing PDOL solid electrolytes with desirable application properties.
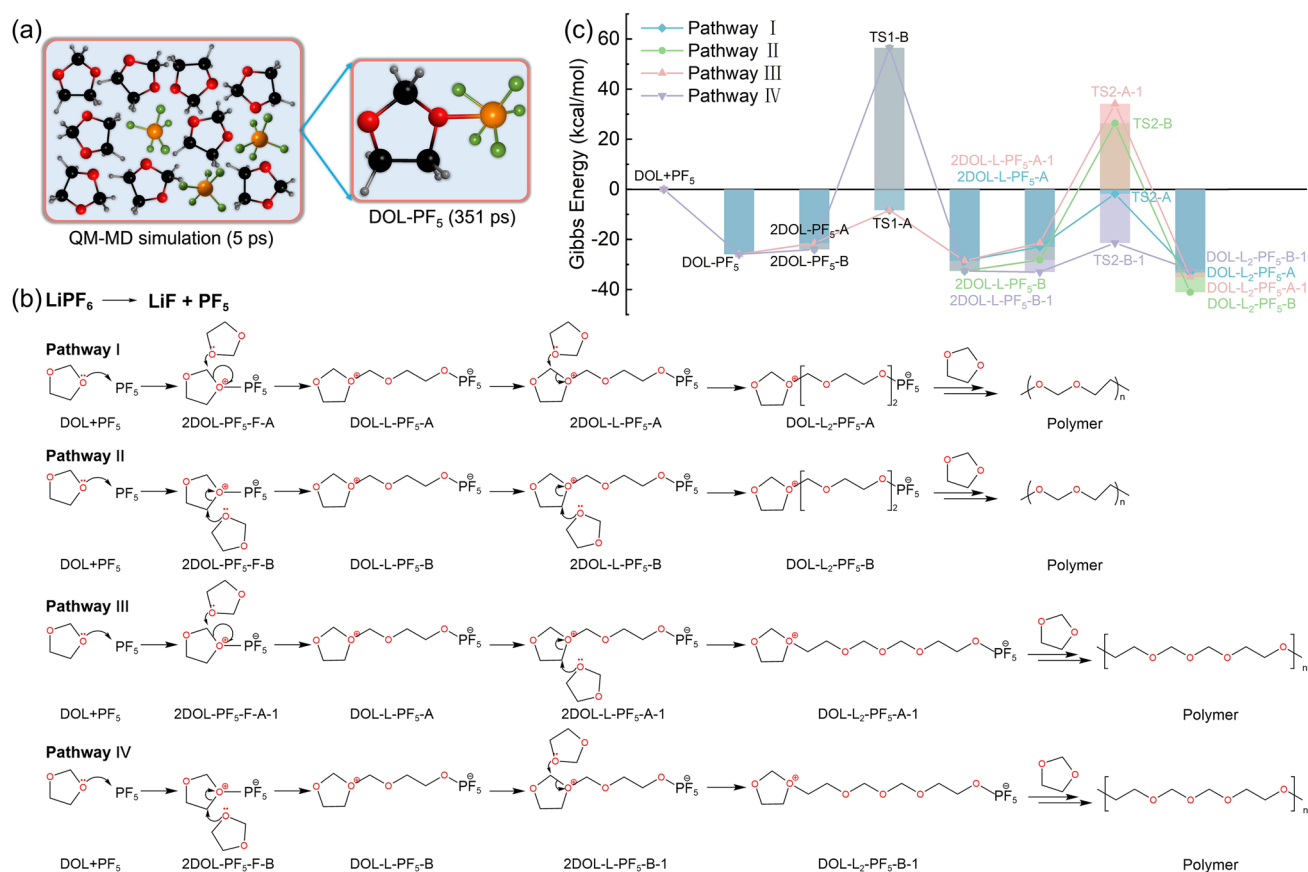
Fig. 5 Schematic diagram of LiPF$_6$-initiated DOL polymerization process. **a** Structure of DOL-PF$_5$ obtained from the 3ps QM-MD simulation of PF$_5$-DOL system. **b** Four possible paths of DOL ring-opening polymerization under the action of PF$_5$ and **c** reaction Gibbs free energy [86]

2.2.1 Polymerization Initiated by Lithium Salt

In the pertinent research on the polymerization of DOL to form PDOL electrolyte, the predominant use of LiPF$_6$ as an initiator is attributed to its high initiation efficiency and excellent cycling performance. Hence, a more comprehensive comprehension of the process of LiPF$_6$-initiated DOL polymerization can enable the derivation of improved DOL polymerization techniques. Tao Cheng [86] used DFT and quantum mechanics (QM) molecular dynamics (MD) simulation to calculate the most possible reaction path for LiPF$_6$-initiated DOL ring-opening polymerization. The QM-MD simulation results, as shown in Fig. 5a, indicate that PF$_6^-$ decomposes into F$^-$ and leaves behind PF$_5$ with free radical properties, while DOL forms a P–O bond with PF$_5$ after 351 fs, and other DOL molecules approach the DOL-PF$_5$ system, which is the initial state of DOL ring-opening reaction. The authors proposed a possible polymerization

path, where LiPF$_6$ first decomposes into LiF and PF$_5$ free radicals, and the lone pair electrons of the O atom in DOL combine with PF$_5$ to form DOL-PF$_5$, where the C–O bond in DOL-PF$_5$ is activated and other approaching DOL molecules attack the C atom to form DOL-L-LF$_5$ via ring-opening reaction. The C–O bond in unopened DOL-L-LF$_5$ is further activated, achieving continuous polymerization. In the above polymerization simulation, there are two types of activated C–O bonds attacked by free DOL: –O–C–O– and –O–C–C–O–, denoted as A and B, respectively. Four more detailed possible polymerization paths can be formed by alternating ring-opening of DOL at the two different C–O bond positions of A and B during the ring-opening process (Fig. 5b). The authors calculated the free energy of the four polymerization reaction pathways and found that the energy barrier of Pathway I that needs to overcome is the lowest (Fig. 5c), making it the most reasonable polymerization path for DOL.
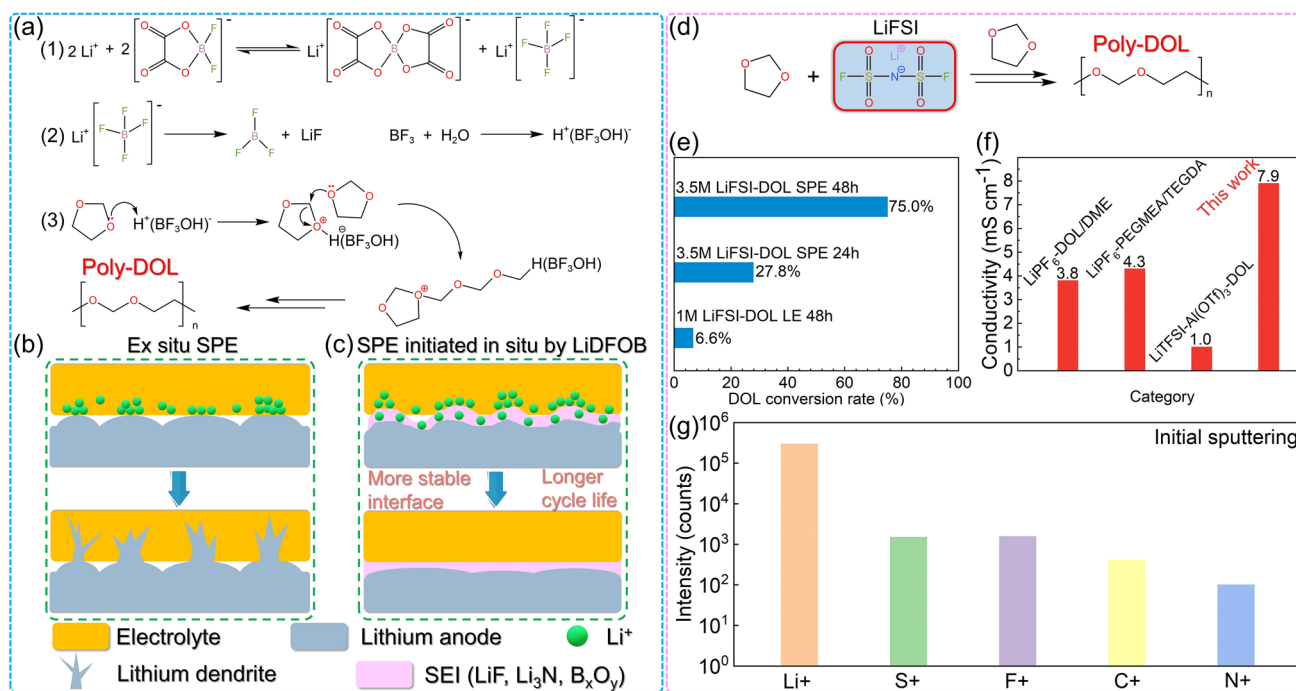
Fig. 6 LiDFOB (LiBF$_4$) or LiFSI initiated DOL polymerization. **a** Schematic illustration of the LiDFOB initiated DOL ring-opening polymerization process. **b** Interphase evolution of ordinary non-in situ polymer electrolytes leads to incomplete interface contact, resulting in uneven ion transport and rapid growth of lithium dendrites [87]. **c** LiDFOB in-situ initiated polymerization of PDOL electrolyte generates SEI rich in boron oxide compounds at the electrolyte/lithium anode interface, which guides ion uniform deposition, resulting in a more stable interphase and longer cycle life. **d** LiFSI initiates DOL ring-opening polymerization process. **e** DOL polymerization conversion rate at different LiFSI content and standing time. **f** Comparison of ionic conductivity of PDOL gel electrolyte initiated by LiFSI with other PDOL electrolytes. **g** TOF–SIMS of C+, F+, S+, N+ and Li+ species on the lithium surface after cycling in the gel electrolyte: species concentration at initial sputtering [77]

Apart from LiPF$_6$, other lithium salts are also widely used as DOL ring-opening initiators due to the trace amounts of protonic acids they generate. Li Yang [87] investigated the mechanism of lithium difluorooxalatoborate (LiDFOB) as a ring-opening initiator. Since LiDFOB often exists partially as LiBF$_4$, its initiation mechanism is analogous to that of LiBF$_4$ (Fig. 6a1). LiBF$_4$ has the ability to generate BF$_3$, and BF$_3$ reacts with H$_2$O to generate H$^+$(BF$_3$OH)$^-$ (Fig. 6a2), which function as potent protonic acids. H$^+$ on H$^+$(BF$_3$OH)$^-$ reacts with the oxygen atom on the DOL ring, initiating the ring-opening polymerization of DOL and generating long chains of PDOL (Fig. 6a3). The Li//Li symmetric battery assembled with LiDFOB initiated polymer electrolyte was tested, which has much longer cycle life than the symmetric battery with ex-situ polymerization. In ex-situ polymerized batteries, there are a large number of defects in the interphase between the electrolyte and the anode, and ions will aggregate at the contact point, accelerating the growth of dendrites (Fig. 6b). In LiDFOB in-situ initiated PDOL batteries, SEI is composed of LiF,

Li$_3$N, and B$_x$O$_y$ derived from initiators, which protect the lithium metal anode while guiding ion uniform deposition, ultimately achieving a more stable interface and longer cycle life (Fig. 6c).

Further, a scheme for initiating DOL ring-opening with high concentration of lithium difluorosulfonamide (LiFSI) has been proposed. The authors were able to initiate the DOL ring-opening reaction with only higher concentration of LiFSI without adding additional lithium salts (Fig. 6d) [77, 88, 89]. With a concentration of 3.5 M LiFSI, the DOL polymerization conversion rate can achieve 75% (Fig. 6e), and the resulting gel electrolyte demonstrates an impressive ionic conductivity of 7.9 mS cm^{-1} (Fig. 6f). The elevated concentration of lithium salt leads to the dissociation of higher concentrations of Li$^+$, thereby playing a crucial role in enhancing Li$^+$ diffusion capability. Time of flight secondary ion mass spectrometry (TOF–SIMS) analysis of the lithium surface SEI cycled in the gel electrolyte shows that the N, F, and S elements from LiFSI gradually decrease as the sputtering time
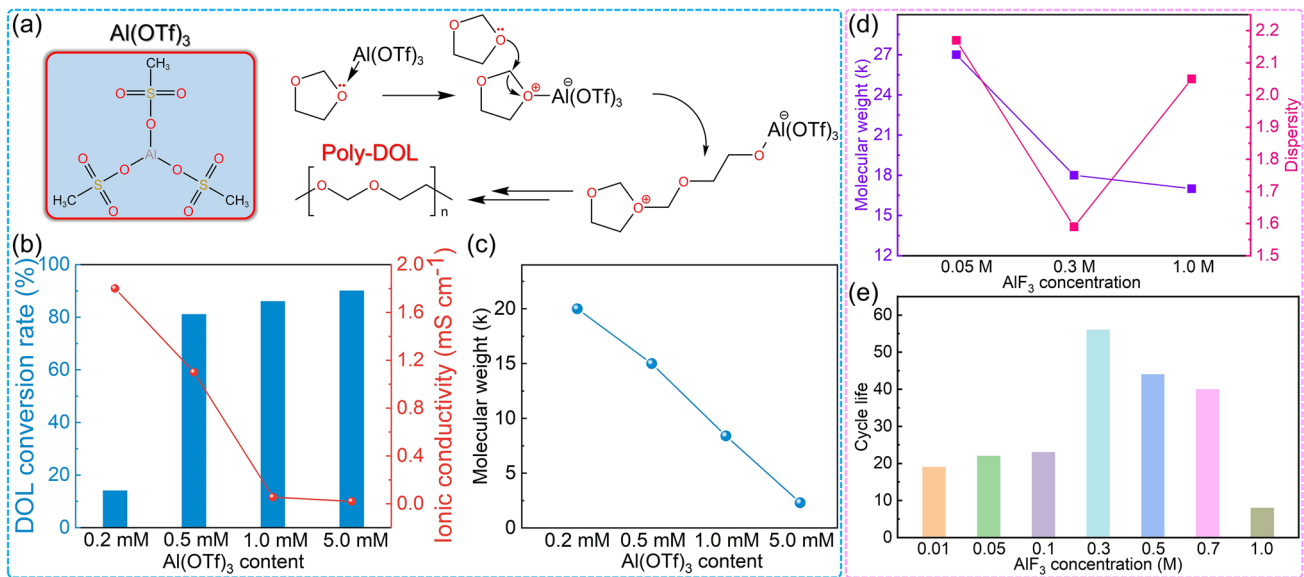
Fig. 7 Aluminum salt initiates DOL polymerization. **a** Mechanism of DOL polymerization initiated by Al(OTf)$_3$. **b** DOL polymerization conversion rate and **c** molecular weight of PDOL initiated by different aluminum salt initiators content [64]. After adding different contents of AlF$_3$, **d** the molecular weight and dispersity of PDOL, and **e** cycle life of PDOL [66]

increases, indicating the formation of a gradient structure SEI (Fig. 6g). It shows that the lithium surface is covered with a LiF-rich SEI layer, which can effectively protect the lithium metal anode.

2.2.2 Polymerization Initiated by Aluminum Salt

Cations in metal salts generally exhibit Lewis acidity and are used as DOL ring-opening initiators [90]. Lynden A.

Archer [64] used trace amounts of aluminum trifluoromethanesulfonate (Al(OTf)$_3$) to initiate in-situ polymerization of DOL. The aluminum cation in Al(OTf)$_3$ exhibits a strong electron-attracting ability and thus preferentially coordinates with the lone pair of electrons on the oxygen atom of the DOL ring. This coordination interaction initiates the ring-opening polymerization of DOL, which subsequently proceeds via a chain-growth mechanism (Fig. 7a). Aluminum salt initiation does not require the involvement of additional trace amounts of water as lithium salt initiation does, and
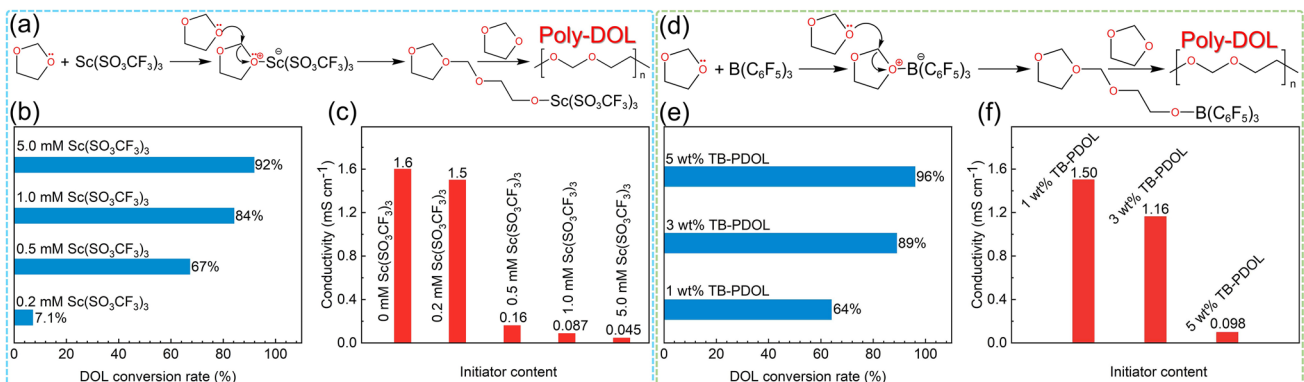

Fig. 8 Scandium salt and TB initiate DOL polymerization. **a** Mechanism of DOL polymerization initiated by Sc(SO$_3$CF$_3$)$_3$. **b** DOL polymerization conversion and **c** ionic conductivity of PDOL electrolyte initiated with different initiator concentrations [92]. **d** TB initiates the DOL polymerization process. **e** DOL polymerization conversion rate and **f** room temperature ionic conductivity initiated by different TB contents [83]

its lower usage indicates its high initiation efficiency. The authors compared the effects of different aluminum salt initiators on the properties of PDOL electrolyte and found that at an initiator concentration of 0.5 mM Al(OTf)$_3$, it simultaneously achieved a polymerization conversion rate up to 81% for DOL and a high ionic conductivity of 1.1 mS cm^{-2} (Fig. 7b). Moreover, the authors discovered that as the concentration of aluminum salt increases, the molecular weight of the polymer decreases due to the rise in initiation sites, leading to a decrease in chain length (Fig. 7c). The in-situ polymerized solid-state LiFePO$_4$ (LFP)//Li batteries maintain high and stable coulombic efficiency during ultra-long cycles.

Building upon this work, the Lynden A. Archer group [66] incorporated AlF$_3$ as a co-initiator with the original Al(OTf)$_3$ to enable application with high-voltage cathode. The addition of AlF$_3$ has a similar effect as the initiator. As its content increases, the molecular weight of PDOL decreases. At a concentration of 0.3 M, the weight average molecular weight is 18 kDa and the dispersion is 1.59 (Fig. 7d). The AlF$_3$ enables the application of PDOL on high-voltage LiNi$_{0.6}$Co$_{0.2}$Mn$_{0.2}$O$_2$ (NCM622) layered

cathode materials. When 0.3 M AlF$_3$ is added, its stable cycle times can reach up to nearly 60 times (Fig. 7e), and the charge/discharge voltage curves also show good cycling stability.

2.2.3 Polymerization Initiated by Other Typical Initiators

Simultaneously serving as a functional additive, initiator is now being used in PDOL electrolytes. Weidong Zhou [79] employed SnF$_2$ as a superior interfacial stabilizer to initiate ring-opening polymerization of DOL. SnF$_2$ can react in situ to generate interphase protective species Li$_x$Sn during battery operation, which can effectively prolong the working life of lithium-ion batteries.

Transition metal salts are also used as alternative initiators for DOL polymerization [91]. Shi Wang [92] employed minute quantities of Sc(SO$_3$CF$_3$)$_3$ to in-situ polymerize and fabricate PDOL solid electrolytes. Similar to traditional aluminum salts, Lewis acidic Sc^{3+} opens the DOL ring and initiates polymerization (Fig. 8a). Comparative experiments showed that with the addition of 1.0 mM Sc(SO$_3$CF$_3$)$_3$, the polymerization conversion rate of DOL
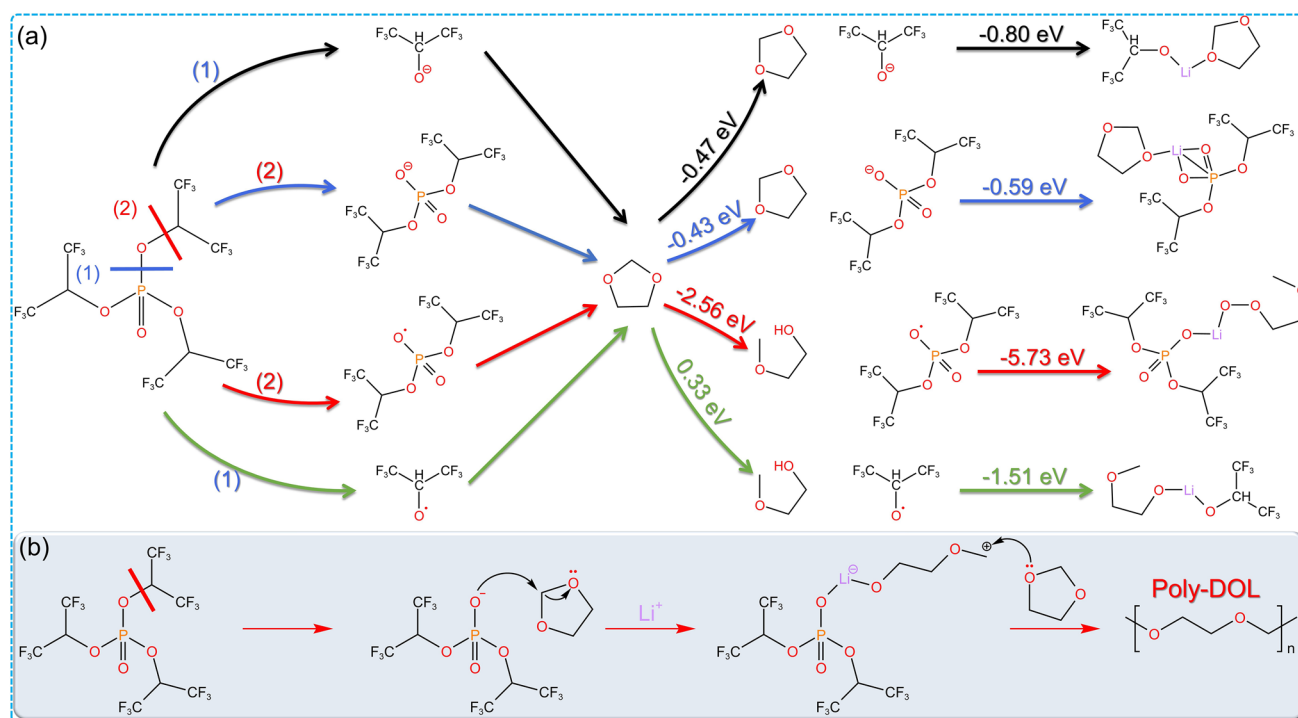

Fig. 9 Nucleophilic polymerization mechanism of DOL. a Some free radicals generated from the decomposition of HFiP and their free energy for ring-opening reactions with DOL. b Schematic diagram of HFiP initiated nucleophilic polymerization of DOL [85]

reaches 84% (Fig. 8b) and the ion conductivity reaches 8.7×10^{-5} S cm^{-1} (Fig. 8c). This trace initiator exhibits high initiation efficiency and good polymerization results.

Except for most salt initiators, organic initiators such as tris(pentafluorophenyl) borane (TB) have also been reported [83]. Its initiation mechanism is also inclined toward salt initiation, and B atom with electron attraction ability will attack the lone electron pairs of oxygen atoms on the DOL ring, leading to the ring-opening of the DOL (Fig. 8d). Incorporation of 3 wt% TB initiator resulted in the attainment of 89% polymerization conversion of DOL (Fig. 8e), while retaining a high room temperature ionic conductivity of 1.16 mS cm^{-1} (Fig. 8f). Surface XPS analysis of the lithium sheet after cycling reveals the formation of a substantial quantity of LiF at the interface, a critical factor in enhancing interfacial stability. Besides, the O–B–O bond present in B$_x$O$_y$ produced by TB decomposition facilitates the creation of cross-linked covalent frameworks, which can culminate in the formation of a more robust SEI.

2.3 Nucleophilic Polymerization of DOL

In the second stage of electrophile-initiated DOL ring-opening polymerization, it also falls under nucleophile initiation: the oxygen atom with a lone pair of electrons on the free DOL ring attacks the carbon atom in the –O–C–O– moiety of the initiator-bound DOL ring, promoting the chain reaction of DOL polymerization. Some initiators can also undergo nucleophilic initiation with the assistance of Li$^+$ in the first stage. Shuting Yang [85] used tris(1,1,1,3,3,3-hexafluoroisopropyl) (HFiP) in situ to initiate DOL ring-opening polymerization by nucleophilic pattern into gel cells. When HFiP is in solution, the P–O and C–O bonds are easily
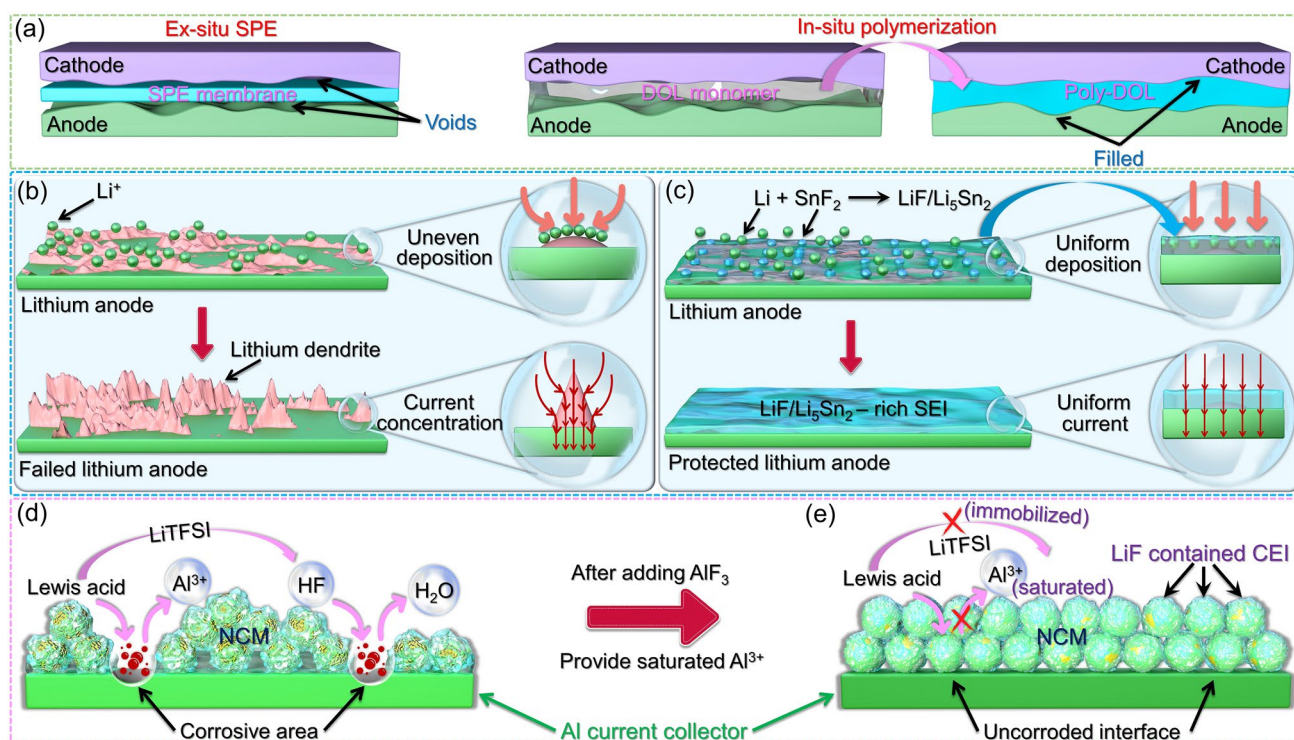

Fig. 10 Contact mode and interface optimization between PDOL electrolyte and solid-state electrode. **a** Differences in interface contact modes between electrolytes and solid-state electrodes in ex-situ polymerization and in-situ polymerization [64]. **b** The uneven deposition of lithium ions on common lithium metal anodes leads to rapid growth of lithium dendrites: in areas where lithium ions are concentrated and deposited, it will further guide the aggregation of ions and currents, leading to the growth of dendrites. **c** In the SnF$_2$-initiated PDOL electrolyte, the initiator undergoes a reaction with lithium to generate Li-Sn alloy, and it then forms a robust LiF/Li$_5$Sn$_2$-rich SEI incorporating LiF. The SEI facilitates the homogeneous deposition of lithium ions and the even distribution of current, providing protection to the lithium metal anode [79]. **d** Mechanism diagram of proton corrosion of aluminum current collector caused by Lewis acid interface reaction. **e** Mechanism diagram of aluminum current collector corrosion inhibition after adding AlF$_3$ [66]

broken [93, 94], and the charged groups after cleavage will attack the oxygen atoms on the DOL ring, leading to DOL ring-opening. DFT calculations show that the ring-opening process under the initiation of cations containing P–O bonds releases 2.56 eV of energy (red line path), which is the most possible initiation mechanism (Fig. 9a). In this pathway, the breaking of the C–O bond generates a negatively charged oxygen atom. This nucleophilic reagent attacks the carbon atom in the –O–C–O– moiety of the DOL ring, opening the ring and initiating the polymerization reaction of DOL, facilitated by the simultaneous action of the electrophilic Li^+ (Fig. 9b). HFiP effectively initiates nucleophilic polymerization of DOL, and its decomposition products have no any impact on the battery, demonstrating excellent stability.

3 Interface of PDOL Electrolyte

The interface engineering between electrolyte and electrode will have a serious impact on the electrochemical performance and operational life of SSLB. Traditional solid-state electrolytes, which have been extensively studied, are often prepared in an ex-situ manner. However, these solid-state electrolytes fail to achieve the wetting effects observed in liquid electrolytes, leading to the formation of significant voids at the interface between the electrolyte and electrode. This phenomenon hampers Li^+ diffusion and contributes to localized current concentration. In contrast, PDOL-based electrolytes can be polymerized from liquid DOL monomers. As a result, introducing DOL monomers and initiators into the battery will enable automatic wetting of the electrode interface. The in-situ liquid–solid transition characteristic of PDOL retains this adaptability, allowing the solid PDOL to effectively fill the interface pores between the electrolyte and electrode, ensuring the continuity of Li^+ diffusion (Fig. 10a).

The energy density advantage of SSLB is related to the lithium metal anode, and the active lithium metal is prone to various side reactions and failure. Constructing SEI protection for lithium metal is an effective method to extend the electrode service life [95–101]. SEI requires high electrochemical stability and ion transport capability, and the reported SEI components mainly include fluorides [95, 102–107] (LiF), nitrides [87, 108] (Li_3N), carbides [107, 109–111] (Li_2CO_3, LiC_x), alloys [79, 112–116] (Li–Cu, Li–Sn, Li–Se), etc. Components such as LiF and Li_3N are mainly derived from the decomposition of lithium salts containing F and N elements, while the formation of carbides is often related to graphite anodes or contact with CO_2 in the air. The alloy composition is mainly related to composite anodes or metal salt additives. To elucidate the protective mechanism of SEI on lithium metal, we employ Li–Sn alloy as an exemplary case. Weidong Zhou [79] pioneered the utilization of SnF_2 initiators to initiate DOL polymerization for the fabrication of solid-state batteries. CV testing was conducted on a Li//Fe battery assembled with PDOL initiated by SnF_2. A small lithiation current was observed at 0.35 and 0.62 V, which could be attributed to the formation of Li_xSn. The X-ray photoelectron spectroscopy (XPS) of F and Sn elements on the surface of the freshly synthesized PDOL electrolyte membrane and the recycled one from Li//Li battery after cycles show that SnF_2 forms a composite SEI enriched with LiF and Li_xSn. Finite element simulation (FES) is utilized to depict the potential field and Li^+ flux distribution at the interface between the electrolyte and lithium metal. In conventional electrolytes, following the initial non-uniform deposition of lithium ions on the surface of the lithium anode, subsequent Li^+ flux is also unevenly distributed, leading to the accelerated growth of lithium dendrites (Fig. 10b). However, the interface electric field of the composite SEI containing Li_5Sn_2/LiF is relatively smoother, resulting in a slower voltage decrease. Due to the significantly higher Li^+ diffusion coefficient of Li_5Sn_2 than that of LiF, Li^+ flux primarily distributes on Li_5Sn_2, which has superior ionic conductivity, while passing through the SEI layer. This facilitates the uniform distribution of Li^+ flux and suppresses the formation of lithium dendrites (Fig. 10c).

The lack of satisfactory high voltage tolerance in DOL is attributed to its instability toward highly charged cathodes, which leads to unwanted reactions. Since DOL monomers inevitably exist in PDOL electrolytes, preventing direct contact between PDOL electrolytes and cathode materials will effectively mitigate undesired side reactions. Coating the cathode [117–119] or constructing a cathode electrolyte interphase (CEI) has been identified as an effective solution. Lynden A. Archer [66] achieved the protection of high-voltage NCM cathodes in PDOL by incorporating AlF_3, and the author also explained the reason why AlF_3 enhances the high-voltage performance. The Lewis acid in the electrolyte generates protons at the interface, which react with the Al_2O_3 on the surface of the aluminum current collector to produce soluble Al^{3+} and react with lithium salt to generate
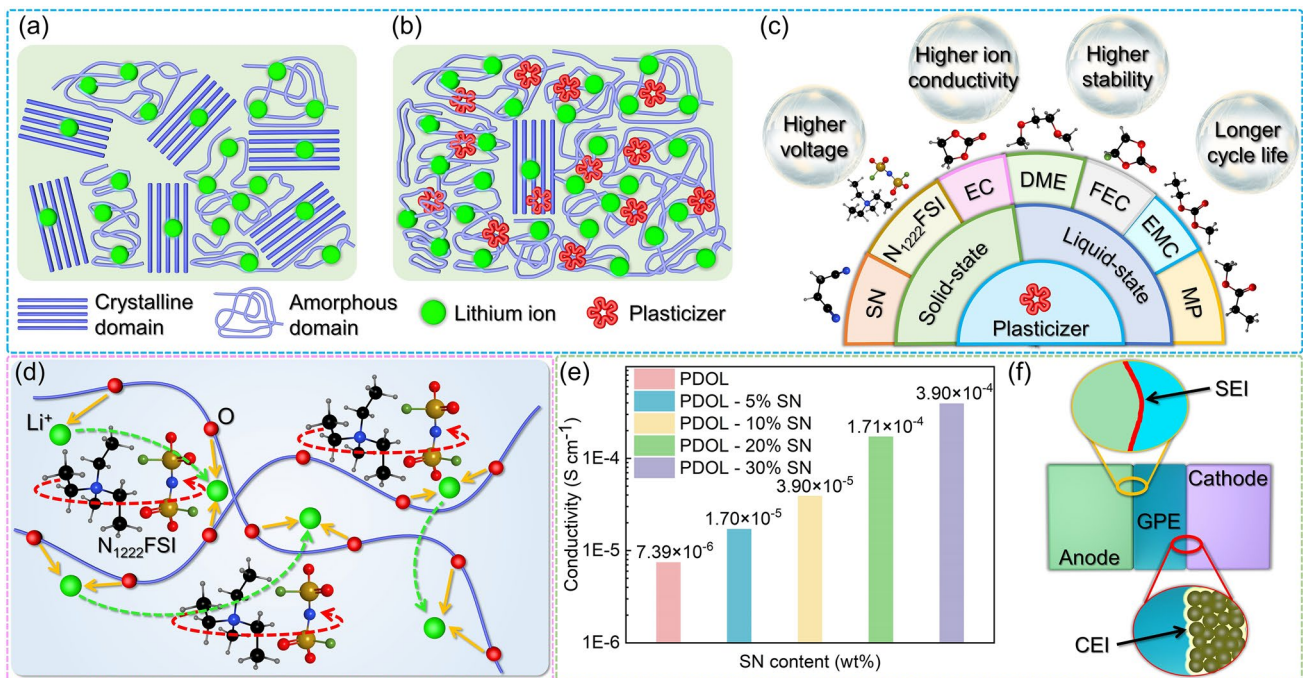
Fig. 11 Improvement of PDOL electrolyte performance by plasticizers. **a** PDOL polymers without plasticizers possess a significant amount of crystalline domains in their structure, which hinders the mobility of polymer chains. **b** The addition of plasticizers to PDOL increases the amorphous domains, facilitating chain segment mobility and resulting in enhanced ion conductivity. **c** The reported types of plasticizers and their enhancements on the performance of PDOL polymers. **d** The internal rotational motion of $N_{1222}FSI$ leads to orientation disorder and the generation of lattice vacancies in PDOL, thereby enhancing ion conductivity [87]. **e** The effect of different SN contents on the ion conductivity of PDOL GPE. **f** The CEI and SEI gradually formed during the cycling process of GPE protect the cathode and anode, respectively [75]

HF. Both reactions can corrode the aluminum current collector (Fig. 10d). The addition of AlF_3 forms a saturated Al^{3+} solution, which prevents the decomposition of Al_2O_3 and immobilizes $TFSI^-$, thereby preventing corrosion of the aluminum current collector (Fig. 10e). Furthermore, the addition of succinonitrile (SN) has been demonstrated to form a thin and stable CEI, which helps maintain the stability of the cathode/PDOL interface and effectively prolong the battery's operational lifespan (Fig. 11f) [75].

4 Composites of PDOL Electrolyte

In the context where SSLB have not yet achieved large-scale commercialization, it is evident that conventional SPE face several unresolved problems. One of the most significant modification strategies for traditional SPE is the addition of additives, which is preparing composite electrolytes. The types of additives mainly include polymer fillers, inorganic fillers, and support scaffolds, among others. The general function of additives is to disrupt the arrangement of polymer segments, reduce the glass transition temperature of polymer, and thereby enhance its room temperature ionic conductivity. The addition of polymer fillers often enhances the toughness of the polymer to improve the interface contact problem. Inorganic fillers are the most commonly used additives to improve the electrochemical performance of polymers. They have significant effects in increasing the polymer's ionic conductivity, widening its electrochemical stability window, and enhancing its thermal stability. The addition of inorganic SiO_2 to pentaerythritol tetraacrylate (PETEA) can significantly enhance its room temperature ionic conductivity, increasing it by an order of magnitude to reach 1.93×10^{-3} S cm^{-1} [104]. When $MoSe_2$ is added to PVDF, the high-voltage tolerance of the SE is increased from 4.3 to 4.7 V [116]. This improvement in voltage stability can enhance the performance and safety of the electrolyte in high-voltage applications. Polymer electrolytes often lack the compressive mechanical strength to resist tearing caused by external pressure. Introducing a support skeleton can effectively address this issue. The support skeleton provides structural integrity and enhances the mechanical

properties of the polymer electrolyte, allowing it to withstand external forces and reduce the risk of tearing or failure. The relatively weak mechanical strength of poly (propylene carbonate) (PPC) prevents it from achieving self-support. However, by incorporating a cellulose support skeleton, the tensile strength of PPC can be enhanced to reach 15 N mm^{-2}, thereby satisfying the application requirements of electrolytes [120]. Conventional SPE has achieved various performance improvements through the addition of additives, which also offer research directions for future SPE modifications.

Despite demonstrating exceptional performance in lithium-ion batteries, PDOL falls short in fully satisfying the practical requirements for its application in terms of volume stability, flexibility, ion conductivity, electrochemical window, high voltage stability, mechanical strength, and thermal stability. Similar to the modification scheme of conventional SPE, combing with other advantageous materials is an effective method to improve its electrochemical properties. Researchers have explored the incorporation of plasticizers, support skeletons, and inorganic fillers to achieve substantial enhancements across various performance parameters. These findings indicate a promising development trajectory for the practical utilization of PDOL in the future.

4.1 Plasticizers

Although the in-situ polymerization approach can significantly enhance the interface contact between the electrolyte and electrode, the polymerization of DOL alone may not be sufficient to achieve optimal results for practical applications. Mainly attributed to two aspects: Firstly, PDOL polymers exhibit partial crystallization, resulting in poor plasticity, which cannot adapt to the defects caused by the repeated volume changes of electrode materials during cycling. Plasticizers can significantly enhance the plastic deformation ability of PDOL electrolytes, actively adapt to changes in electrode volume, and reduce defects. Secondly, the high degree of polymerization of PDOL and its ionic conductivity do not satisfy the requirements for high energy density batteries. The large number of crystalline domains inside PDOL hinder the peristalsis of the chain segments, and the migration of ions cannot meet the application requirements (Fig. 11a). The introduction of plasticizers increases the

amorphous domains of PDOL polymers, leading to a significant enhancement in ion conductivity (Fig. 11b).

The reported plasticizers for PDOL electrolytes encompass two categories: solid-state and liquid-state, both of which primarily consist of small molecule monomers. Solid plasticizers will retain more of the advantages of PDOL polymers as solid electrolytes, while liquid plasticizers exhibit excellent performance in improving the ionic conductivity of PDOL polymers. Higher electrode stability and higher ion conductivity are the most prominent contributions of plasticizers to PDOL polymers. Furthermore, certain plasticizers have demonstrated the ability to enhance high voltage tolerance and prolong the cycle life of PDOL polymers, further optimizing their overall performance (Fig. 11c). Plasticizers are simple and extremely effective in improving the performance of PDOL polymers.

Li Yang [87] incorporated the organic ionic plastic crystal triethylmethylammonium bis (fluorosulfonyl) imide (N_{1222}FSI) into the PDOL electrolyte and evaluated the impact of various plasticizers on the performance of PDOL. As the N_{1222}FSI content increased, the researchers observed a corresponding rise in ion conductivity and a decrease in the degree of polymerization of the electrolyte. The researchers posit that the addition of N_{1222}FSI to the PDOL electrolyte provides two pathways for Li$^+$ transport. One is facilitated by the coordination/dissociation of N_{1222}FSI with the oxygen atoms in PDOL, while the other is enabled by the orientation disorder and lattice vacancies generated by ion rotation inside N_{1222}FSI (Fig. 11d). These mechanisms are considered to be the primary factors contributing to the observed improvement in the ion conductivity of the polymer when compared to pure PDOL electrolyte. Furthermore, at additive levels between 0 and 40 wt%, the electrochemical stability window of the PDOL electrolyte surpasses 5.8 V, thereby providing a solid foundation for practical applications.

1,2-dimethoxyethane (DME) has been extensively used as a plasticizer for PDOL electrolytes and has shown favorable balance performance [58, 59, 63, 67, 77, 85, 121]. Maoxiang Jing [122] investigated in detail the effect of DME addition on PDOL polymerization conversion and found that with increasing DME content, the polymerization conversion of DOL decreased. The Arrhenius equation was employed by the author to fit and compute the activation energy at varying ratios, based on the ion conductivity measurements at different temperatures. The analysis revealed that the addition of DME to PDOL electrolyte reduces the lowest activation

energy to as low as 0.1 eV, providing greater facilitation of Li$^+$ diffusion across a broader temperature range. However, the introduction of a higher concentration of small molecule DME into PDOL-based polymer electrolytes has been shown to decrease the electrochemical stability window. Therefore, careful regulation of the DOL and DME ratio is essential to achieve a balance between ion conductivity and electrochemical stability window.

The plastic crystalline plasticizer, SN, has been found to enhance the ion conductivity of PDOL polymer [75]. It was observed that the ion conductivity of PDOL steadily increased as the SN content increased (Fig. 11e). The ion conductivity measurements conducted at varying temperatures revealed that the addition of SN resulted in a lower ion migration barrier and higher ion conductivity. Nevertheless, akin to small molecule plasticizers like DME, the incorporation of SN into PDOL was found to decrease the

electrochemical stability window. The author balanced the performance of both and chose to add 30 wt% SN to achieve better comprehensive performance (Fig. 11e). Furthermore, the authors discovered that the cathode in PDOL with the addition of SN forms a thin and stable CEI after cycling (Fig. 11f). This interphase reduced the Li$^+$ diffusion barrier and effectively suppressed interface side reactions. Several studies have further added fluoroethylene carbonate (FEC) [81, 123–125] on the basis of adding SN, and have observed further improvements in both the ionic conductivity and electrochemical stability window of the polymer.

In the traditional liquid electrolyte system, a combination of ethylene carbonate (EC) and ethyl methyl carbonate (EMC) is used to dissolve the DOL ring-opening initiator Sc(OTf)$_3$ and employed as plasticizers for PDOL polymer [126, 127]. Pre-dissolved initiators can initiate DOL polymerization more uniformly to prevent local polymerization.
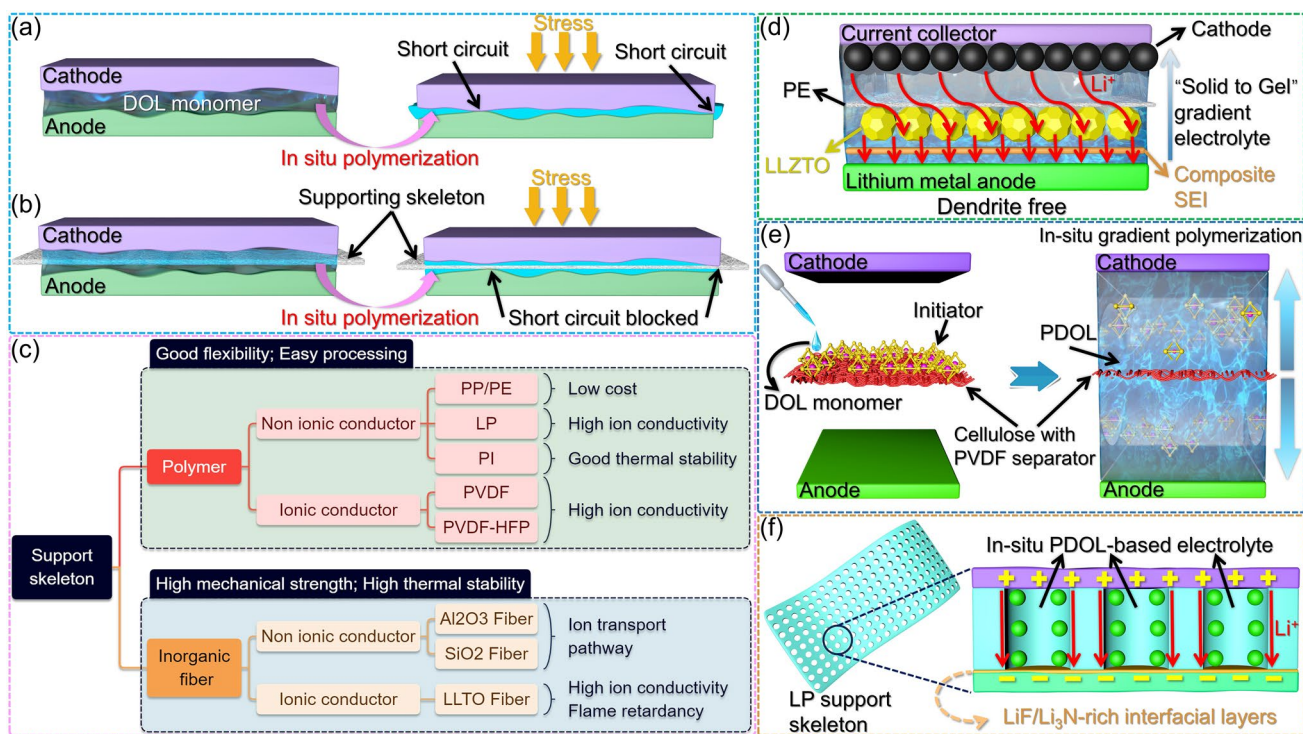

Fig. 12 Function and classification of support skeleton. **a** In the absence of a support skeleton, the electrode may come into contact and experience short circuits under external pressure during the in-situ polymerization process of DOL. **b** The presence of support skeletons effectively serves as a mechanical barrier, preventing electrode contact and mitigating the risk of short circuits during the in-situ polymerization process. **c** The types of support skeletons and their corresponding advantages, they can be broadly categorized into two main groups: polymer-based and inorganic-based materials. **d** Schematic diagram of the battery structure after DOL gradient polymerization initiated by modified PE, the densely polymerized PDOL solid electrolyte adjacent to the anode serves as a protective barrier for the lithium metal, while the partially polymerized PDOL gel electrolyte in close proximity to the porous cathode effectively permeates and infiltrates the electrode [131]. **e** Schematic diagram of bidirectional gradient polymerization of DOL on modified cellulose paper [132]. **f** Schematic diagram of the interphase layer between electrolyte and LP to enhance ion conductivity [76]

The plasticizing properties of EC/EMC can also significantly enhance the ion conductivity of the polymer. In addition, using the low-melting plasticizer methyl propionate (MP) [128] and adjusting the ratio between DOL, MP, and LiTFSI can optimize the ion conductivity, with the highest room-temperature ion conductivity exceeding 2.9 mS cm^{-1}. The PDOL-MP composite electrolyte demonstrates suitability for the assembly of high-voltage NCM811//Li batteries, enabling the attainment of a relatively stable cycling performance.

4.2 Support Skeleton

The high ionic conductivity exhibited by the PDOL polymer at room temperature is attributed to its comparatively lower glass transition temperature, which correlates with its reduced mechanical strength under the same conditions. As a consequence of its low mechanical strength, the aforementioned electrolyte is inadequate for effectively separating the cathode and anode, thereby compromising the battery's stability under external pressure and exacerbating the issue of dendrite growth of the lithium metal anode, all of which are indispensable factors for the optimal performance of a lithium-ion battery (Fig. 12a). Consequently, it is imperative to reinforce the PDOL polymer with a robust support skeleton, capable of maintaining electrode isolation even in the face of external pressure or deformation. This measure is vital for sustaining normal operation under challenging environmental conditions (Fig. 12b). The support skeletons mentioned in literatures primarily encompass polymer and inorganic materials, each boasting distinct advantages. Polymer skeletons are renowned for their superior flexibility and ease of processing, while inorganic skeletons exhibit higher mechanical strength and ion conductivity. These materials can be further classified into ionic conductors and non-ionic conductors based on their capacity to conduct Li$^+$ ions. Within their compositions, these materials possess unique functionalities that cater to a diverse array of requirements (Fig. 12c). The performance of the battery varies depending on the choice of the support material, and thus, identifying a functionally balanced support skeleton is a crucial research avenue for achieving high-performance PDOL polymer solid electrolytes.

4.2.1 Polymer Support Skeleton

Polyethylene (PE) and polypropylene (PP) separators are commonly employed as support skeletons for traditional liquid batteries thanks to their stable electrochemical properties and good mechanical strength [59, 64, 129, 130]. Maoxiang Jing [131] implemented additional processing steps to the PE separator to satisfy the requirements of PDOL-based solid-state batteries. Initially, the PE separator was treated with a LiPF$_6$ solution to facilitate the loading of initiator for DOL polymerization, following which a high concentration of fast ion conductor Li$_{6.4}$La$_3$Zr$_{1.4}$Ta$_{0.6}$O$_{12}$ (LLZTO) solution was applied to one side of the separator. After drying, a PE separator loaded with LLZTO layer (facing lithium metal anode) and initiator was obtained. Direct injection of DOL and LiTFSI into a modified PE separator in cells for in-situ polymerization results in the gradient polymerization of PDOL electrolyte from PE to both sides. The incompletely polymerized gel PDOL can effectively infiltrate the porous cathode, whereas the lithium metal anode side features a highly robust and ion-conductive LLZTO layer that facilitates the uniform deposition of ions and stifles dendrite growth (Fig. 12d). The author draws the stress–strain curve of the electrolyte membrane through tensile testing and found that the fracture strength of the electrolyte is as high as 55.0 MPa.

Conventional PP and PE separators often encounter a challenge of inadequate wettability of DOL, which can be significantly improved by using porous cellulose membranes with high mechanical properties and low cost. Hongfa Xiang [132] utilized PVDF as a binder to load γ-Al$_2$O$_3$ and aluminum salt initiators onto cellulose paper. The incorporation of γ-Al$_2$O$_3$ as an inorganic filler significantly enhanced the mechanical strength and electrochemical performance of the resulting polymer. In the process of cell assembly, the modified cellulose paper was directly infused with DOL + LiTFSI solution on both sides. The initiator presents on the cellulose gradually dissolved and triggered the DOL polymerization, and the ensuing gradient diffusion polymerization resulted in improved interfacial contact between the electrode and the electrolyte (Fig. 12e).

Lithium nitrate-containing mesoporous polymer (LP) is an ideal support skeleton for PDOL polymer electrolytes, with its pores filled with in-situ polymerized PDOL [76]. During the cycling, a LiF/Li$_3$N-rich interphase layer with high ion conductivity will be formed between the electrolyte

and LP, which will improve the stability of Li$^+$ transport. The pores of LP provide a dedicated channel for Li$^+$ transport, and the electrolyte/LP interface forms a fast Li$^+$ transport path, which can effectively improve the ion conductivity of the electrolyte (Fig. 12f). The polymerized PDOL-LP electrolyte membrane exhibits transparency and has a thickness of merely 12 µm. Yet it boasts a high tensile fracture strength of up to 3.5 MPa, which is even 30 times higher than that of conventional PEO-based electrolytes, underscoring its exceptional value as a support skeleton. The researchers fabricated an LFP//Li pouch cell featuring LP-supported PDOL electrolyte and subjected the cell to 1000 bending cycles with a radius of 5 mm. The voltage curves during the bending process exhibited typical voltage behavior and remained unaffected by the bending behavior. Furthermore, the pouch cell could supply power normally in flat, 90° bent, cut, and punctured states, demonstrating excellent performance of LP in terms of toughness and safety. On the other hand, the additional non-conductive support skeleton will occupy a portion of the volume of the conductive polymer, which may lead to a reduction in the ion transport medium.

Augmenting the affinity between the support skeleton and PDOL polymer facilitates the formation of a stable polymer electrolyte membrane. Additionally, a relatively higher porosity can accommodate more conductive polymer, rather than the non-conductive supporting skeleton occupying most of the volume. Jianhua Yan [67] used electrospinning method to prepare a porous polyimide nanofiber (PI-NF) film as a supporting skeleton. First, polyamic acid (PAA) was rendered into a PAA solution and electrospun into PAA-NF at high voltage. Then, the PAA-NF was heated to form a yellow PI-NF film by intramolecular dehydration of the PAA closed-loop molecule. Then, DOL/DME solution containing an initiator and LiTFSI was dropped onto the PI-NF, and the DOL was ring-open polymerized to form a quasi-solid-state electrolyte. The stress–strain curve demonstrated that PI-NF possessed a remarkable tensile strength of 12.3 MPa and a high strain of 89%. The intensive crosslinking between PDOL and PI-NF considerably augmented the tensile strength of the PI quasi solid electrolyte (PIQSE) film to 31 MPa. In comparison with the PP-supported QSE, the PI-supported QSE exhibited superior thermal stability. Specifically, the PIQSE remained structurally intact when
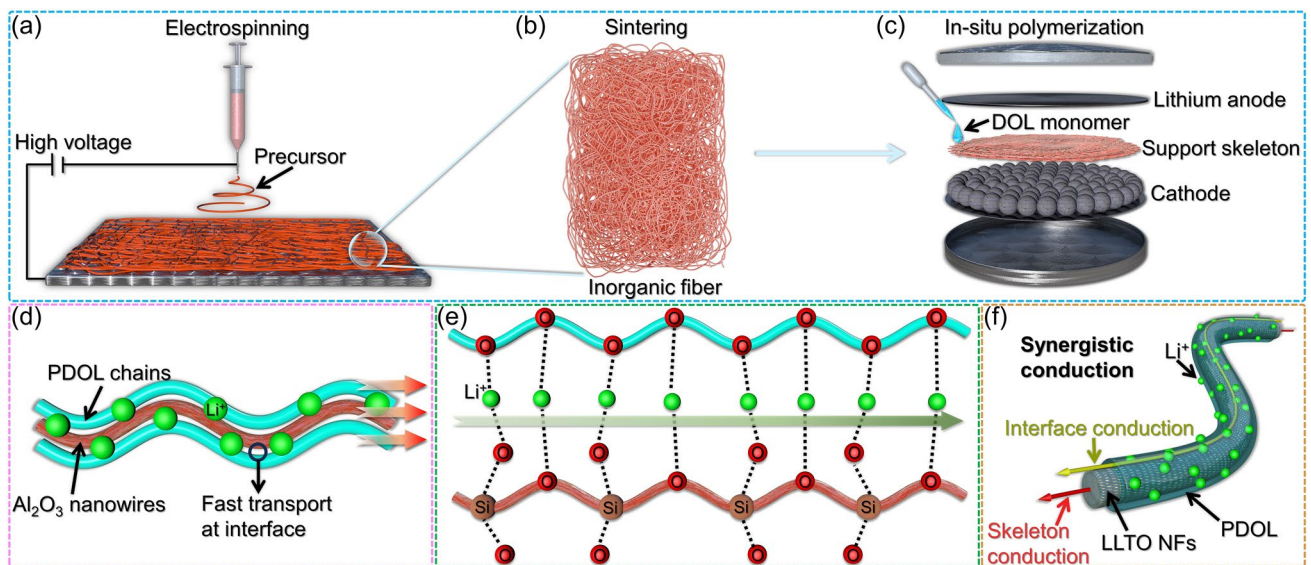

Fig. 13 Inorganic fiber materials as PDOL support skeleton. **a** The precursor of inorganic materials is electrospun to prepare a fiber network at high voltage. **b** Inorganic material precursors are sintered to form inorganic fiber support skeletons. **c** Structural diagram of a battery supported by an inorganic fiber skeleton through in-situ polymerization. **d** The interface between Al$_2$O$_3$ nanowires and PDOL polymer segments constructs a high-speed ion transport channel, accelerating Li$^+$ transport [92]. **e** The oxygen atoms of PDOL and the Si–O bonds of SiO$_2$ collectively create a highly efficient pathway for Li$^+$ migration [139]. **f** LLTO NFs possess Li$^+$ transport capability, while the interface between LLTO NFs and PDOL also exhibits high-speed Li$^+$ transport capability, the synergistic conduction of both components enhances the overall ionic conductivity of the electrolyte [80]

subjected to a temperature of 160 ℃, whereas the PPQSE underwent complete melting. Nonetheless, the SE prepared by this method encounter challenges such as complex process procedures.

The support skeleton with ionic conductivity can cooperate with PDOL to simultaneously transport Li$^+$, which can improve the overall ionic conductivity of polymer electrolytes. PVDF-HFP is widely used as polymer solid electrolyte because of its high electrochemical stability and ionic conductivity [41, 133–136]. Yulong Xu [123] prepared porous PVDF-HFP membranes using a simple pouring method. SEM images showed that the membrane surface and cross-section were uniformly distributed with a large number of evenly sized pores (with a diameter of about 1 μm). This porous PVDF-HFP has excellent liquid electrolyte retention ability and absorbs a large amount of Li$^+$, ensuring sufficient Li$^+$ migration ability. Gang Sui [137] further modified the electrospun PVDF-HFP fiber membrane with dopamine (PDA). PDA can form hydrogen bonds with in-situ polymerized PDOL to further enhance the mechanical strength of the electrolyte membrane. Contact angle tests showed that DOL had the best wettability on the PDA/PVDF-HFP skeleton, which is a prerequisite for forming a complete ion transport pathway. Importantly, the tensile strength of the PDOL@PDA/PVDF-HFP electrolyte membrane obtained by these modifications reached 10.1 MPa (152% improvement compared to PVDF), which can meet the requirements of production processes and practical applications.

4.2.2 Inorganic Fibers Support Skeleton

Inorganic materials possess higher tensile and compressive mechanical strength than polymers, and polymer electrolytes supported by them are expected to have higher stability and safety. Electrospinning is often used to prepare highly porous inorganic membrane materials to accommodate sufficient ion-conductive polymers (Fig. 13a–c) [110, 111, 138]. What is more, the interface between inorganic materials and polymers usually exhibits faster ion transport, and fibrous inorganic materials can guide ion transport and enhance ion transfer efficiency [7]. Moreover, the high thermal stability of inorganic materials can resist thermal decomposition at high temperatures, thereby improving the safety performance of batteries. Therefore, the application of inorganic

materials in polymer electrolytes has broad prospects for development.

Shi Wang [92] utilized electrospinning to fabricate an Al$_2$O$_3$ ceramic fiber skeleton, which was implemented as a supportive matrix for PDOL gel electrolyte. The ceramic fiber membrane constructed a new Li$^+$ transmission channel at ceramic/polymer interface (Fig. 13d). The prepared PDOL/Al$_2$O$_3$ membrane can achieve free-standing and has good toughness. Zhicong Shi [139] prepared a three-dimensional SiO$_2$ nanofiber framework as support skeleton by electrospinning. SiO$_2$ has better thermal stability, mechanical strength, and electrochemical stability than polymer [140, 141]. The interface between SiO$_2$ and PDOL established a swift Li$^+$ transmission pathway (Fig. 13e), resulting in a composite electrolyte with an ion conductivity of 1.68×10^{-4} S cm^{-1} at 30 °C.

Inorganic materials with inherent Li$^+$ transport capabilities as supporting skeletons have two ion conduction channels, bulk ion transport and interface ion transport, thus their ion conductivity has greater advantages [142]. Yue-E Miao [80] prepared a three-dimensional fast ion conductor La$_{0.56}$Li$_{0.33}$TiO$_3$ (LLTO) nanofibers (NFs)-supported in-situ polymerized PDOL polymer electrolyte by electrospinning. The porous fibers with a diameter of approximately 500 nm, and the pores are completely filled after in-situ polymerization. In comparison with a pure PDOL membrane, the LLTO-supported electrolyte membrane demonstrates a substantially diminished risk of thermal runaway, and displays self-extinguishing properties during capacitive discharge. Combined with the inherent ion conductivity of LLTO fibers and the interface ion high-speed transmission channel constructed (Fig. 13f), the room temperature ion conductivity of the composite electrolyte was significantly increased to 6.6×10^{-4} S cm^{-1}, which made a substantial contribution to the application of PDOL-based polymer electrolytes.

The inorganic support skeleton that brings various advantages inevitably reduces the toughness of PDOL polymers, which may limit their application in flexible batteries. Therefore, SE membranes should find a balance point in the long-term conflict between strength and toughness to achieve optimal comprehensive performance. Xueliang Sun [143] referred to "Ceramic-in-Polymer" and "Polymer-in-Ceramic" as representatives of toughness and strength, respectively. A sandwich-structured composite electrolyte was prepared with a high-strength support structure in the middle as "Polymer-in-Ceramic" and high-toughness
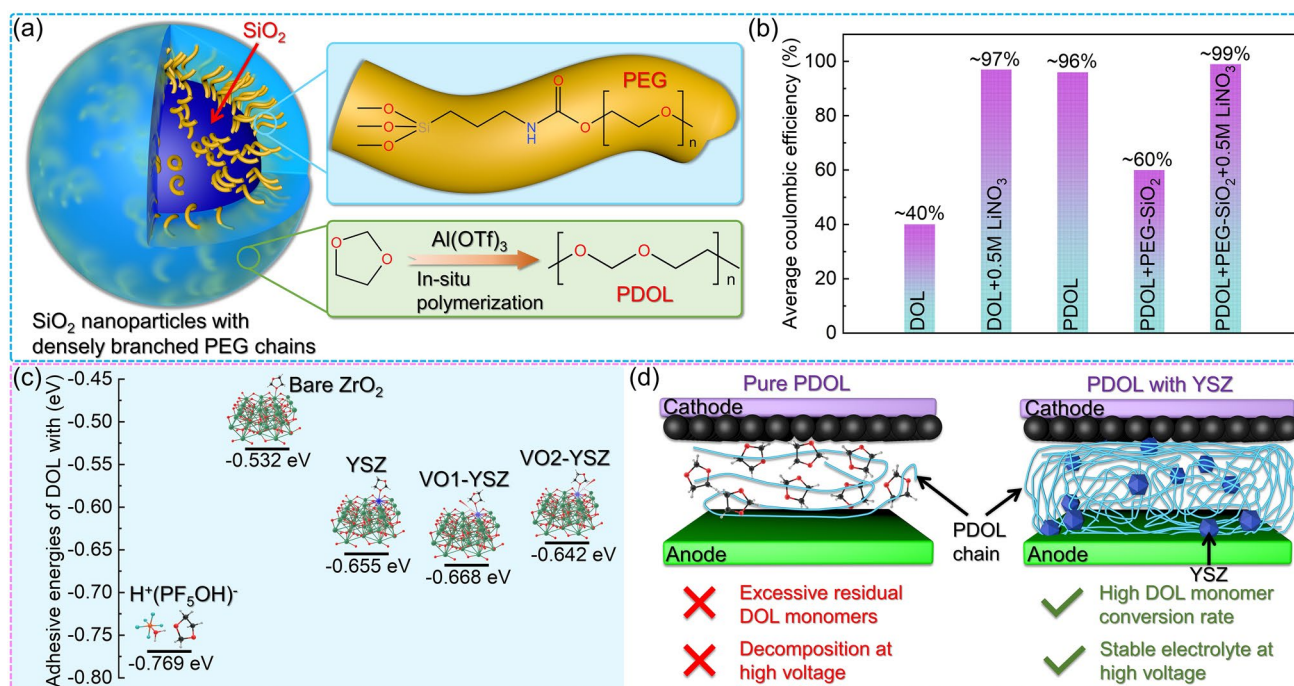
Fig. 14 Inorganic materials enhance the performance of PDOL. **a** Schematic diagram of PEG grafting on the surface of SiO_2 and co-crystallization with PDOL. **b** Average coulombic efficiency for 200 cycles of Li//Cu battery assembled with PDOL-SiO_2 composite electrolyte [151]. **c** DFT calculated ring-opening binding energy of DOL monomer with initiator, ZrO_2, zirconium atom on YSZ and oxygen vacancy on YSZ. **d** The auxiliary activation of YSZ substantially enhances the monomer conversion rate of DOL, resulting in a significant improvement in the high voltage capability of the electrolyte, this enhancement enables the attainment of a long service life that aligns with high voltage cathode materials [68]

components on both sides as "Ceramic-in-Polymer" to meet the dual requirements of strength and toughness in the electrolyte. This structural design may be one of the potential solutions in the future to balance the conflicting demands of strength and toughness in polymer electrolytes.

4.3 Inorganic Fillers

Polymer solid electrolytes can often be improved in various aspects such as room temperature ion conductivity, electrochemical stability and mechanical strength through composites with inorganic materials [144]. Numerous relevant studies have confirmed the remarkable impact of lithium fast ion conductors and inert inorganic materials on enhancing the performance of polymer electrolytes [143, 145–149]. The interface between the developed inorganic material surface and PDOL exhibits lower Li^+ diffusion energy and promotes ion diffusion ability at the interface [150].

Lynden A. Archer [151] used aluminum salts to initiate the ring-opening polymerization of DOL in situ to adapt to the electrolyte–electrode interface, and modified it with densely branched PEG chain-nanoparticles of SiO_2 (Fig. 14a). The nanoscale SiO_2 can be stably dispersed in the DOL monomer solution, and the high dielectric constant of SiO_2 can improve the dielectric and flame retardancy of the PDOL-based composite electrolyte. The grafted PEG provides a spatial barrier to prevent filler aggregation, and increases the amorphous region of PDOL by co-crystallizing with PDOL. Not to mention, the interface-grafted PEG also has Li^+ conduction ability. The synergistic effect of the ion conductivity of the PDOL bulk phase and the interphase improves the overall ion conductivity of the PDOL-SiO_2 composite electrolyte, reaching 1.5 mS cm^{-1} at room temperature. A Li//Cu battery was constructed and subjected to cycling tests, where the PDOL-SiO_2 composite electrolyte exhibited an exceptional level of stability with a coulombic efficiency of 99% for 200 cycles (Fig. 14b).

The inability of DOL monomers to withstand high voltage has always been criticized, so electrolytes containing large amounts of DOL monomers often have poor cycling performance in high voltage battery systems, which is one of the most important means to achieve high energy density batteries in the future [152]. Early DOL-based electrolytes could only be used in battery systems below 3.0 V (such as lithium-sulfur batteries) [56, 153, 154], later the polymerization of DOL was carried out to improve the high voltage resistance of PDOL, which can be applied to battery systems around 4.0 V (such as LFP batteries) [59]. Both theoretical and experimental studies have demonstrated that the DOL monomer in PDOL restricts its application in high voltage batteries. Therefore, enhancing the DOL monomer conversion rate during the DOL ring-opening polymerization process is a crucial factor in improving the stability of PDOL electrolytes in high voltage batteries. One of

the primary reasons for DOL ring-opening is the presence of a Lewis acid. Yttrium stabilized zirconia (YSZ) is considered a strong Lewis acid materials are highly susceptible to oxygen vacancies and have been reported as effective inorganic fillers for polymer solid electrolytes [49, 150, 155]. Xiangming He [68] prepared PDOL-YSZ composite solid electrolyte by YSZ assisted catalytic DOL ring-opening polymerization. DFT calculations showed that the zirconium atoms and oxygen vacancies on YSZ have similar ring-opening binding energies to the initiator (Fig. 14c), which can effectively promote DOL ring-opening polymerization. The residual rate of DOL monomer in PDOL electrolyte with YSZ addition was only 1.5%, and the decomposition voltage was as high as 5.2 V (Fig. 14d). The assembled high voltage NCM622//Li battery (2.8–4.3 V) maintained a capacity retention rate of 74% after 800 cycles

Table 2 Cyclic performance of PDOL polymer electrolyte matched with different cathodes

Battery type	Cathode materials	Initiator	Additive	Voltage range (V)	Initial specific capacity (mAh g^{-1})	Rate (C)	Cycle number	Capacity retention (%)	Refs
Lithium-sulfur batteries	Sulfur	ACNTP	–	1.7–3.0	683	1.0	400	66.5	[56]
	Sulfur	$LiPF_6$	DME	1.8–3.0	1005	0.5	500	73.7	[58]
	Sulfur	$LiPF_6$	DME/Al_2O_3	1.8–3.0	1102	0.1	200	73.0	[59]
	Sulfur	LiFSI	DME	1.7–2.8	910	0.2	300	75.5	[77]
	Sulfur	HFiP	DME	1.8–2.8	1025	0.5	500	68.1	[85]
	Sulfur	$LiPF_6$	DME	1.7–2.8	870	0.1	500	45.0	[163]
Lithium-ion batteries	LFP	$LiPF_6$	DME	2.5–4.0	137	0.5	700	95.6	[58]
	LFP	LiDFOB	SN	2.5–4.0	127	1.0	1 000	83.55	[75]
	LFP	LiFSI	DME	2.5–3.8	147	1.0	500	69.3	[77]
	LFP	$Sc(OTf)_3$	–	2.5–4.0	155	0.5	200	83.5	[91]
	LFP	$Al(OTf)_3$	PDA	3–3.75	145	1.0	200	87.1	[137]
	LFP	$Y(OTf)_3$	LLZTO	2.8–3.8	135	0.2	200	~70.0	[142]
	LFP	$LiPF_6$	PI/DME	2.5–3.7	152	0.5	200	91.8	[67]
	LFP	$Mg(OTf)_2$	FEC	2.8–4.2	127	1.0	2 000	94.0	[81]
	LFP	LiDFOB	FEC/SN	2.8–4.3	142	2.0	1 000	95.0	[123]
	NCM622	$LiPF_6$	DME	2.8–4.3	165	0.1	100	90.9	[58]
	NCM622	$Al(OTf)_3$	AlF_3	2.8–4.2	160	0.5	30	80	[66]
	NCM622	$LiPF_6$	–	2.8–4.3	138	0.5	300	85	[129]
	NCM622	$LiPF_6$	YSZ	2.8–4.3	165	0.5	800	74	[68]
	NCM523	LiFSI	–	3.0–4.3	136	0.1	100	94	[89]
	NCM811	LiDFOB	FEC/SN	2.8–4.3	145	0.2	100	70.6	[123]
	NCM83	$S(C_2H_4O_4)$	–	2.8–4.5	205	0.5	100	89.5	[84]
	LCO	LiDFOB	SN	2.8–4.3	140	0.1	60	57.1	[75]
	LMFP	$LiBF_4$	TTE	3.0–4.3	130	0.2	100	~90	[76]
Sodium-ion batteries	NVP	$Al(OTf)_3$	FEC	2.0–3.8	99	5.0	2 000	93.6	[125]

at room temperature at 0.5 C, demonstrating excellent high voltage stability.

Zilong Zhuang [156] synthesized a graphitic-C_3N_4 (g-C_3N_4)-PDOL composite electrolyte layer in-situ on the lithium metal surface. The flexible PDOL can physically separate the electrolyte from the corrosion of lithium metal, while g-C_3N_4 can enhance the ion conductivity of the composite layer, guide ion uniform deposition, and suppress dendrite growth.

5 PDOL-Based Electrolytes for Solid-State Lithium Batteries

PDOL-based polymer electrolytes have demonstrated notable enhancements in multiple electrochemical properties through various aforementioned modification methods. Furthermore, it demonstrates exceptional operational stability at ambient temperature in both conventional lithium-ion and lithium-sulfur battery systems. In addition, to broaden its application range, researchers have further enhanced its battery performance, encompassing safety and low-temperature environmental performance, by incorporating functional additives. This advancement has facilitated the practical utilization of PDOL polymer electrolytes in lithium batteries.

5.1 Cycle Performance at Ambient Temperature

We have summarized one of the most important application indicators of some typical reported PDOL-based SSLBs, which is their cycling performance under different cathode materials and operating voltages (Table 2). In early research on DOL and PDOL, due to their poor high voltage resistance, they were mainly used in lithium sulfur battery systems. The most outstanding performance among them is a capacity retention rate of 73.7% after 500 cycles at 0.5 C, and the initial specific capacity also exceeds 1000 mAh g^{-1} [58]. Nevertheless, the practical application of lithium-sulfur batteries encounters notable challenges due to their low operating voltage and areal loading. Consequently, in order to facilitate the widespread utilization of PDOL polymers, it is imperative to enhance their high voltage resistance to achieve compatibility with mainstream high voltage cathode materials.

Subsequent investigations have seen researchers employing varied initiators to synthesize PDOL polymer electrolytes with higher DOL monomer conversion rates. This approach has led to improved high voltage resistance and enabled their application compatibility with LFP cathodes. Yang Guanming [91] utilized $Sc(OTf)_3$ as the initiator to synthesize PDOL-based electrolyte and achieve a matched SSLB configuration with LFP cathodes. The SSLB underwent 200 charge–discharge cycles within a voltage range of 2.5–4.0 V, demonstrating an impressive capacity retention rate of 83.5%. Moreover, the cycling performance was further enhanced by incorporating additives, including reported compounds such as DME, SN, PDA, $Li_{6.4}La_3Zr_{1.4}Ta_{0.6}O_{12}$ (LLZTO), PI, FEC, etc. Li Zhenchao [81] achieved the most prolonged cycle life in the reported PDOL system by employing $Mg(OTf)_2$ as the initiator for polymerization and incorporating FEC as an additive. Remarkably, after undergoing 2000 charge–discharge cycles at a rate of 1.0 C within the voltage range of 2.8–4.2 V, the PDOL-based electrolyte exhibited an outstanding capacity retention rate of 94%. This remarkable performance highlights its promising application prospects. Under the current conditions of PDOL polymerization process and materials, LFP with relatively low operating voltage has been reported the most as the cathode material for PDOL polymer electrolytes, and it lays the foundation for practical application in terms of cycle life.

In order to meet the demanding energy density requirements of future SSLB, it is imperative for PDOL polymers to satisfy heightened operating voltage criteria. Nonetheless, PDOL encounters substantial challenges when it comes to compatibility with high-voltage cathode materials. Zhao Chen-Zi [66] successfully developed a CEI by incorporating AlF_3 into the system to inhibit the undesirable reaction between cathode materials and electrolyte. This breakthrough allowed for stable cycling of batteries utilizing PDOL and NCM622 cathode materials. However, the cycling performance, although adequate, did not meet the desired standards for practical applications. Further investigations have confirmed that the lack of high voltage resistance in PDOL systems can be attributed to the interaction between non-polymerized DOL monomers and cathode materials. Therefore, enhancing the conversion rate of DOL monomers is recognized as one of the most effective approaches to improve high voltage resistance capability. He Xiangming [68] successfully synthesized a PDOL solid electrolyte with an impressive DOL monomer

conversion rate of up to 98.5% using open environment polymerization and YSZ-assisted initiation. When combined with the NCMM622 cathode material, the PDOL-based SSLB underwent 800 cycles within the voltage range of 2.8–4.3 V, with a remarkable capacity retention rate of 74%. This highly favorable cycling performance stands as one of the best reported for high-voltage PDOL-based SSLB systems, highlighting the potential of PDOL polymers for future application in high energy density SSLBs. In addition, PDOL polymers can also be matched with various cathode materials, including $LiNi_{0.5}Co_{0.2}Mn_{0.3}O_2$ (NCM523), $LiNi_{0.8}Co_{0.1}Mn_{0.1}O_2$ (NCM811), $LiNi_{0.83}Co_{0.11}Mn_{0.06}O_2$ (NCM83), $LiCoO_2$ (LCO), $LiMn_{0.8}Fe_{0.2}PO_4$ (LMFP), and even the cathode material $Na_3V_2(PO_4)_3$ (NVP) for sodium ion batteries, showing broad application prospects.

In addition, compared with other SPEs that may achieve practical applications such as PEO-based [157], PVDF-based [158], siloxane-based [159], sulfone-based [160], etc., PDOL-based electrolytes demonstrate notable advantages in terms of electrochemical performance and stability. Significantly, PDOL stands out by being prepared through an in-situ liquid–solid transition process, thereby eliminating interphase defects that commonly arise from direct solid–solid contact between solid electrolytes and solid electrodes. A more detailed comparison further unveils a host of compelling advantages. The glass transition temperature of PEO is around 60 °C, which means that its ion conductivity needs to be at high temperatures to meet the application requirements, which is incongruent with the operating environment of the majority of batteries. Additionally, PEO is incompatible with high-voltage cathode materials and unsuitable for integration into high-energy density lithium-ion battery systems [157]. PDOL-based electrolytes can operate normally at room temperature or even low temperatures, meeting the practical application needs of lithium-ion batteries. PDOL-based electrolytes with high monomer conversion rates can match high voltage NCM cathodes, providing higher energy density. The Siloxane-based electrolyte achieved stable 1000 cycles when matched with the LFP cathode, but similar to the problem faced by PEO, its electrochemical stability window is below 4.2 V [159], making it unable to match with higher voltage cathode materials. Both PVDF-based and sulfur-based electrolytes have high-voltage resistance and can be matched with NCM cathodes, indicating promising application prospects. However, PVDF-based electrolytes often require the addition of

additional solvents to enhance their ionic conductivity [161, 162], which increases their unsafe factors. Sulfone-based [160] electrolytes are mainly composed of liquid components, and the construction of LiF-rich SEI to protect lithium metal anode achieves excellent long-life cycles. However, their advantages in moving toward high safety, high energy density, and leak free SSLB will lag behind solid electrolytes such as PDOL-based electrolytes.

5.2 Safety and Thermal Stability

There have been numerous explosion and combustion safety accidents caused by thermal runaway in traditional liquid batteries, and solid electrolytes are widely regarded as one of the best solutions to solve this safety hazard in the future [164]. Yet, the decomposition temperature of pure PDOL is relatively low, and it cannot maintain a stable state after being heated. Therefore, there is still much room for improvement in terms of safety.

Chenglin Yan [65] synthesized a thermoresponsive solid electrolyte by copolymerizing DOL with poly(lithium allyl-sulfide) (PLAS), which manifests autonomous reaction with temperature. In the event of a potentially hazardous temperature rise in the battery, the electrolyte will irreversibly block the transport of ions, effectively curbing any further thermal accumulation. The thermoresponsive electrolyte is crosslinked by PDOL and PLAS and exhibits good toughness. When the battery is assembled with the thermoresponsive electrolyte, it is found that the battery can discharge normally and stably before reaching the dangerous temperature. While, in the event of a temperature surge exceeding 70 °C, the battery's operation is automatically suspended, which effectively eliminates any potential for further temperature escalation and thermal runaway.

Aside from preventing thermal accumulation from the source, flame-retardant PDOL-based electrolytes can also be designed to ensure that no combustion occurs after thermal runaway [84]. Yunhui Huang [83] used TB to initiate the polymerization of DOL to prepare a flame-retardant-type polymer electrolyte. TB produces fluorine radicals as an efficient flame retardant, which can realize a non-flammable electrolyte. The PP separator quickly burns and disappears when heated, while the PDOL-TB electrolyte maintains good non-flammability during heating. When the flame-retardant electrolyte is assembled into a flexible pouch cell,
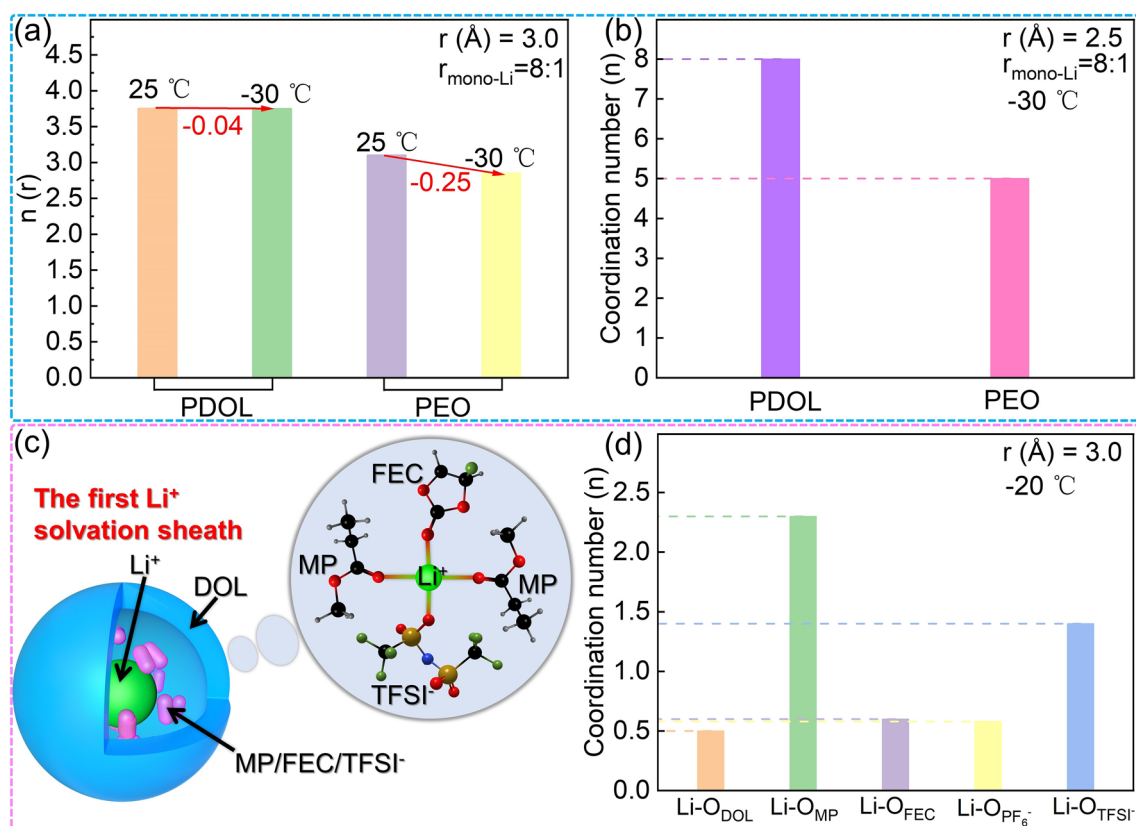
Fig. 15 Low temperature performance of PDOL. **a** Li–O integrated RDF of PDOL and PEO ($r_{mono-Li}=8:1$). **b** Local coordination number of Li$^+$ and O atoms of PDOL and PEO at −30 °C ($r_{mono-Li}=8:1$) [166]. **c** The first Li$^+$ solvation sheath and snapshot of QSPE from MD simulation for QSPE at -20 °C. **d** The coordination numbers of Li$^+$ in the first solvation shell (3 Å) in QSPE at −20 °C [128]

the battery did not experience short-circuiting or burning after being cut twice and can continue to supply power normally. The battery exhibits great advantages in maintaining high safety under sudden destructive conditions.

5.3 Low-Temperature Performance

The ionic conductivity of solid-state electrolytes is one of the biggest challenges that hinders their application, especially at low temperatures where the issue is more severe [165]. Tao Qian [166] compared the ion conductivity of PDOL and PEO at room temperature and low temperature based on MD simulations. The Li–O radial distribution function of PDOL and PEO shows that the coordination number of PDOL is higher than that of PEO within a distance of 3 Å, indicating that Li$^+$ in PDOL can contact more oxygen atoms (Fig. 15a). At low temperature (−30 °C), the coordination number of PEO decreases by 0.25, while that of PDOL only decreases

by 0.04 (Fig. 15a). At a temperature of −30 °C, PDOL exhibits coordination of 2 Li$^+$ with 8 oxygen atoms within a 2.5 Å distance, whereas PEO shows coordination of 2 Li$^+$ with only 5 oxygen atoms (Fig. 15b). At high Li$^+$ concentration, the advantage of PDOL is even more pronounced. The differential scanning calorimetry (DSC) analysis of liquid electrolyte, PEO and PDOL showed that PDOL has a very low glass transition temperature and no melting temperature, indicating that it has amorphous properties, which is also the reason for its high low-temperature ionic conductivity. Testing has shown that the room temperature ionic conductivity of PDOL reaches 1.2×10^{-4} S cm^{-1}, which remains at 1.1×10^{-4} S cm^{-1} even when reduced to -40 °C. This is much higher than PEO and lays the theoretical foundation for the application of PDOL at low temperatures.

Francesco Ciucci [128] developed a quasi-solid polymer electrolyte (QSPE) based on PDOL and incorporating FEC and MP as plasticizers, which can be cycled at low temperature, and investigated its operating mechanism. The MD

simulation snapshot of QSPE is shown in Fig. 15c (within the gray circle), the radial distribution function shows that the first Li$^+$ solvated sheath is mainly composed of FEC, MP and TFSI$^-$ (Fig. 15c). The MP coordination number of Li$^+$ in the first solvated layer is 2.3, and the TFSI$^-$ is 1.4 (Fig. 15d). The MP with low viscosity and melting point ensures the Li$^+$ diffusion capacity of QSPE at low temperatures. The specific capacity of the NCM811//Li battery assembled with QSPE cycled at 0.2 C for 100 cycles at -20 °C was 109 mAh g^{-1}, and the charge–discharge voltage curves at low temperature showed normal Li$^+$ intercalation/deintercalation ability without destructive polarization.

5.4 Instability of PDOL Electrolyte

In-situ polymerization of PDOL to form polymer electrolytes often results in the coexistence of DOL monomers due to incomplete conversion. Investigating the decomposition factors of these two components can provide insights into the factors influencing the stability of PDOL-based polymer electrolytes. Perla B. Balbuena [167] used ab initio Molecular Dynamics (AIMD) to simulate the decomposition of DOL monomers on charged Li electrolyte interfaces.

Simulation shows that DOL generates $(C_2H_4)_2^-$ and $OCH_2O_2^-$ radicals through a 4-electron mechanism and the cleavage of the double C–O bond. Unfortunately, the previously generated $(C_2H_4)_2^-$ will further initiate the continuation of DOL ring-opening and damage to DOL, and as the external electric field increases, the activation barrier decreases, making this reaction easier to proceed. Therefore, the existence of DOL monomer in the high voltage system will affect the electrochemical stability of the electrolyte.

While extensive research has demonstrated the electrochemical stability of PDOL at high voltages, its thermal decomposition mechanism remains unclear. Weidong Zhou [79] analyzed the composition of decomposition gases produced by PDOL electrolyte upon heating to 110 °C using gas chromatography-mass spectrometry (GC–MS). The results showed that the C–O bond of PDOL is prone to breakage at high temperatures, producing formaldehyde and potentially recombining to form dioxane, trioxane, and other cyclic products, and even recombining to form DOL monomers, all of which pose serious threats to the safety of the battery. Therefore, the thermal stability of PDOL-based polymer electrolytes needs to be further improved, which is the foundation of their future applications.
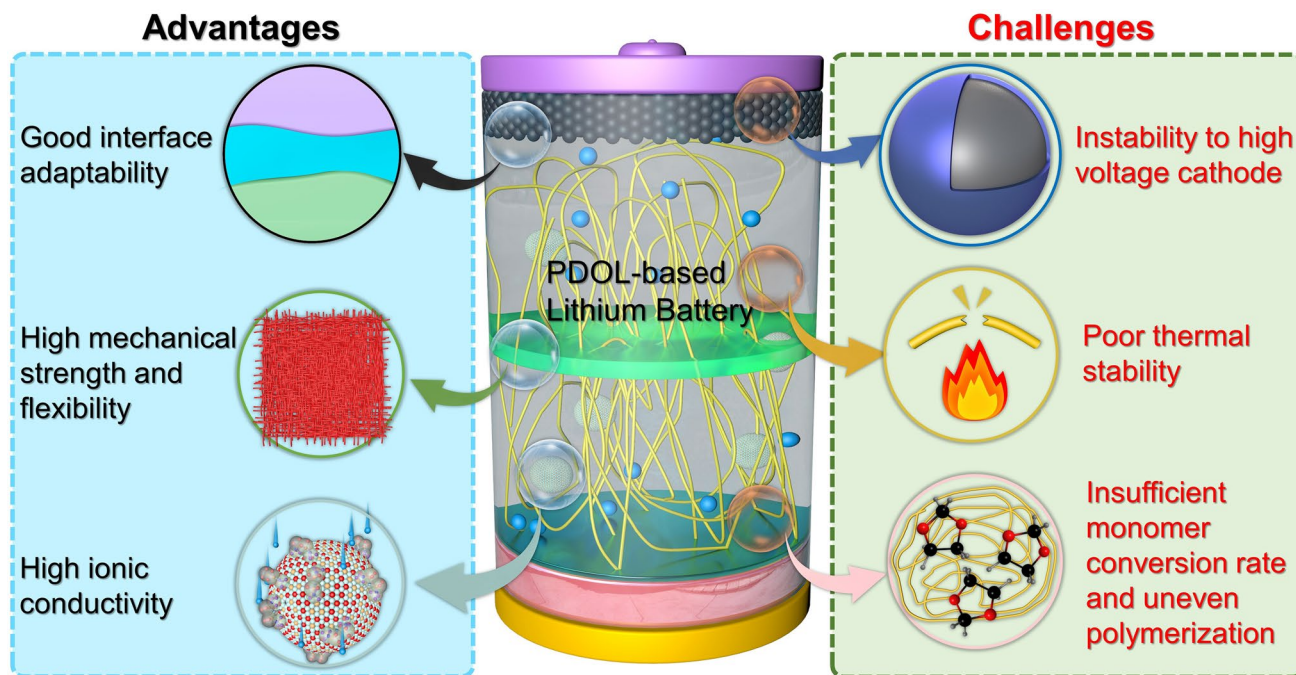

Fig. 16 Advantages of PDOL polymer electrolytes and existing challenges in practical applications

6 Perspectives and Conclusions

PDOL polymer electrolytes have demonstrated numerous advantages over conventional solid-state electrolytes in limited research. These advantages serve as the foundation for their prospective practical applications, primarily encompassing (Fig. 16 left):

(1) The electrolyte derived from in-situ polymerization exhibits enhanced adaptability to the electrolyte–electrode interface, thereby facilitating seamless ion transport;

(2) Diverse support skeletons significantly enhance the mechanical robustness and flexibility of PDOL polymer electrolytes, enabling them to effectively accommodate external pressure and deformation. This ensures the secure operation of batteries and broadens the application scope of PDOL-based lithium batteries.

(3) The addition of plasticizers and inorganic fillers increases the amorphous region of PDOL polymers, thereby yielding heightened ionic conductivity and enabling satisfactory functionality even under exceedingly low temperatures.

Moreover, PDOL polymer electrolytes exhibit good performance in electrochemical stability windows, safety, and Li⁺ transference number. Despite this, its current performance is not yet sufficient for commercial applications. Based on the current reported performance of PDOL-based polymers, we have summarized the remaining challenges and future improvement directions (Fig. 16 right):

(1) Unpolymerized DOL monomers are susceptible to decomposition and electrolyte damage upon encountering high voltage cathodes. This can be mitigated by reducing the DOL monomer content or constructing a robust CEI;

(2) The thermal stability of PDOL polymer segments is insufficient, rendering them susceptible to decomposition with increasing temperature. To enhance heat resistance, future investigations can focus on reinforcing the strength of chain segments through cross-linking polymerization techniques;

(3) In situ polymerization lacks the ability to ensure complete monomer conversion and precise control over the uniformity of polymer distribution. Moving forward, it is imperative to explore more efficient initiators that contain high uniformity of solubility.

Furthermore, one of the future research directions is the modification of the PDOL chain segment itself. Previous studies have demonstrated significant improvement in the electrochemical performance of PDOL by copolymerizing DOL with other monomers to form block or cross-linked polymers [69, 76, 168–170]. The glass transition temperature of block copolymers is frequently dictated by the polymer with the lower temperature [171–174]. Therefore, copolymerizing DOL with other monomers can effectively impede the crystallization of the copolymer and enhance the mobility of the chain segments [69, 169, 170]. Lin Li [168] copolymerized DOL and trioxymethylene as monomers in a ratio of 8/2, resulting in Li⁺ diffusion coefficients of up to 7.37×10^{-13} m² s⁻¹ and ion conductivity of 3.56×10^{-4} S cm⁻¹. The product of copolymerization modification of DOL monomer with 1,3-bis(3-glycidoxypropyl)tetramethyldisiloxane has higher thermal stability and wider electrochemical stability window. The silicon containing SEI layer generated during the cycling process can effectively protect the lithium metal anode [170]. Furthermore, the copolymerization products of DOL with trimethylolpropane tris[3-(2-methyl-1-aziridine) propionate] [169], trimethylolpropane triglycidyl ether [76] significantly improved their electrochemical stability, thermal stability, and ionic conductivity. In the future, the addition of functional monomers may bring broader applications to the PDOL chain segment, such as higher mechanical strength, improved safety, and increased ionic conductivity.

To obtain a more comprehensive understanding of the mechanisms underlying PDOL polymer electrolytes, particularly in terms of ion conductivity, electrochemical stability, and other factors, further investigation is warranted regarding their entropy contribution. More work should be carried out (such as concentration, temperature, additives, etc.) to explore the contribution of entropy and the influence on kinetics, product outcomes and controls thereof.

In conclusion, although PDOL solid electrolyte still faces some problems to be solved, the traditional successful polymer electrolyte research methods can be borrowed to improve its performance further. The current monomer polymerization conversion rate of PDOL has reached 98.5%, and can be cycled more than 2000 times when matched with LFP cathode [81], and more than 800 times when matched with high-voltage NCM cathode [68]. This article provides a more specific and in-depth introduction to PDOL-based SPE prepared by in-situ

polymerization compared to previous reviews. This review analyzes opportunities and challenges of PDOL electrolytes toward practical application for polymer solid-state lithium batteries in terms of polymerization mechanism, composite modification, and battery applications, and proposes further research prospects for their future potential commercialization. This will provide theoretical guidance and expand the scope of ideas for further research and practical applications of PDOL polymer electrolytes. With the emergence of future materials and the application of novel characterization techniques such as neutron scattering and coherent-THz spectroscopy, the challenges faced by PDOL polymers may be resolved, enabling them to achieve practical commercial applications.

Author contributions Prof. LW, Prof. MJ and Prof. XH figured out the idea of this paper and guide the formation of paper framework. Dr. HY drafted this manuscript. All authors help to revise and completed this draft and finalized this paper professionally.

Declarations

Conflict of interest The authors declare no interest conflict. They have no known competing financial interests or personal relationships that could have appeared to influence the work reported in this paper.

References

1. J.B. Goodenough, K.-S. Park, The Li-ion rechargeable battery: a perspective. J. Am. Chem. Soc. **135**, 1167–1176 (2013). https://doi.org/10.1021/ja3091438
2. Y. Wu, W. Wang, J. Ming, M. Li, L. Xie et al., An exploration of new energy storage system: high energy density, high safety, and fast charging lithium ion battery. Adv. Funct. Mater. **29**, 1805978 (2019). https://doi.org/10.1002/adfm.201805978
3. H. Wang, L. Sheng, G. Yasin, L. Wang, H. Xu et al., Reviewing the current status and development of polymer electrolytes for solid-state lithium batteries. Energy Storage Mater. **33**, 188–215 (2020). https://doi.org/10.1016/j.ensm.2020.08.014
4. H.-J. Ha, E.-H. Kil, Y.H. Kwon, J.Y. Kim, C.K. Lee et al., UV-curable semi-interpenetrating polymer network-integrated, highly bendable plastic crystal composite electrolytes for shape-conformable all-solid-state lithium ion batteries. Energy Environ. Sci. **5**, 6491–6499 (2012). https://doi.org/10.1039/C2EE03025J
5. A.L. Ahmad, U.R. Farooqui, N.A. Hamid, Synthesis and characterization of porous poly(vinylidene fluoride-co-hexafluoro propylene) (PVDF-co-HFP)/poly(aniline) (PANI)/graphene oxide (GO) ternary hybrid polymer electrolyte membrane. Electrochim. Acta **283**, 842–849 (2018). https://doi.org/10.1016/j.electacta.2018.07.001
6. P. Ding, Z. Lin, X. Guo, L. Wu, Y. Wang et al., Polymer electrolytes and interfaces in solid-state lithium metal batteries. Mater. Today **51**, 449–474 (2021). https://doi.org/10.1016/j.mattod.2021.08.005
7. K.K. Fu, Y. Gong, J. Dai, A. Gong, X. Han et al., Flexible, solid-state, ion-conducting membrane with 3D garnet nanofiber networks for lithium batteries. Proc. Natl. Acad. Sci. U.S.A. **113**, 7094–7099 (2016). https://doi.org/10.1073/pnas.1600422113
8. X. Ban, W. Zhang, N. Chen, C. Sun, A high-performance and durable poly(ethylene oxide)-based composite solid electrolyte for all solid-state lithium battery. J. Phys. Chem. C **122**, 9852–9858 (2018). https://doi.org/10.1021/acs.jpcc.8b02556
9. B.K. Choi, Y.W. Kim, H.K. Shin, Ionic conduction in PEO–PAN blend polymer electrolytes. Electrochim. Acta **45**, 1371–1374 (2000). https://doi.org/10.1016/s0013-4686(99)00345-x
10. J. Feng, L. Wang, Y. Chen, P. Wang, H. Zhang et al., PEO based polymer-ceramic hybrid solid electrolytes: a review. Nano Converg. **8**, 2 (2021). https://doi.org/10.1186/s40580-020-00252-5
11. Y. Liu, S. Gorgutsa, C. Santato, M. Skorobogatiy, Flexible, solid electrolyte-based lithium battery composed of LiFePO$_4$ cathode and Li$_4$Ti$_5$O$_{12}$ anode for applications in smart textiles. J. Electrochem. Soc. **159**, A349–A356 (2012). https://doi.org/10.1149/2.020204jes
12. M.-K. Song, J.-Y. Cho, B.W. Cho, H.-W. Rhee, Characterization of UV-cured gel polymer electrolytes for rechargeable

lithium batteries. J. Power. Sources **110**, 209–215 (2002). https://doi.org/10.1016/s0378-7753(02)00258-6

13. F. Liu, N. Awanis Hashim, Y. Liu, M.R. Moghareh Abed, K. Li, Progress in the production and modification of PVDF membranes. J. Membr. Sci. **375**, 1–27 (2011). https://doi.org/10.1016/j.memsci.2011.03.014

14. F. Chen, J. Luo, M.-X. Jing, J. Li, Z.-H. Huang et al., A sandwich structure composite solid electrolyte with enhanced interface stability and electrochemical properties for solid-state lithium batteries. J. Electrochem. Soc. **168**, 070513 (2021). https://doi.org/10.1149/1945-7111/ac0f89

15. J. Hu, P. He, B. Zhang, B. Wang, L.-Z. Fan, Porous film host-derived 3D composite polymer electrolyte for high-voltage solid state lithium batteries. Energy Storage Mater. **26**, 283–289 (2020). https://doi.org/10.1016/j.ensm.2020.01.006

16. K. Yang, L. Chen, J. Ma, C. Lai, Y. Huang et al., Stable interface chemistry and multiple ion transport of composite electrolyte contribute to ultra-long cycling solid-state $LiNi_{0.8}Co_{0.1}Mn_{0.1}O_2$/lithium metal batteries. Angew. Chem. Int. Ed. **60**, 24668–24675 (2021). https://doi.org/10.1002/anie.202110917

17. A. Rahimpour, M. Jahanshahi, A. Mollahosseini, B. Rajaeian, Structural and performance properties of UV-assisted TiO_2 deposited nano-composite PVDF/SPES membranes. Desalination **285**, 31–38 (2011). https://doi.org/10.1016/j.desal.2011.09.026

18. S. Golcuk, A.E. Muftuoglu, S.U. Celik, A. Bozkurt, Synthesis and characterization of polymer electrolyte membranes based on PVDF and styrene via photoinduced grafting. J. Polym. Res. **20**, 144 (2013). https://doi.org/10.1007/s10965-013-0144-2

19. S. Rajendran, Experimental investigations on PAN–PEO hybrid polymer electrolytes. Solid State Ion. **130**, 143–148 (2000). https://doi.org/10.1016/s0167-2738(00)00283-6

20. X. He, J. Ren, L. Wang, W. Pu, C. Jiang et al., Synthesis of $PAN/SnCl_2$ composite as Li-ion battery anode material. Ionics **12**, 323–326 (2006). https://doi.org/10.1007/s11581-006-0051-1

21. W.-P. Chen, H. Duan, J.-L. Shi, Y. Qian, J. Wan et al., Bridging interparticle Li^+ conduction in a soft ceramic oxide electrolyte. J. Am. Chem. Soc. **143**, 5717–5726 (2021). https://doi.org/10.1021/jacs.0c12965

22. X. He, Q. Shi, X. Zhou, C. Wan, C. Jiang, In situ composite of nano SiO_2–P(VDF-HFP) porous polymer electrolytes for Li-ion batteries. Electrochim. Acta **51**, 1069–1075 (2005). https://doi.org/10.1016/j.electacta.2005.05.048

23. J. Cao, L. Wang, M. Fang, Y. Shang, L. Deng et al., Interfacial compatibility of gel polymer electrolyte and electrode on performance of Li-ion battery. Electrochim. Acta **114**, 527–532 (2013). https://doi.org/10.1016/j.electacta.2013.10.052

24. J. Cao, L. Wang, M. Fang, X. He, J. Li et al., Structure and electrochemical properties of composite polymer electrolyte based on poly vinylidene fluoride–hexafluoropropylene/titania–poly(methyl methacrylate) for lithium-ion batteries. J. Power. Sources **246**, 499–504 (2014). https://doi.org/10.1016/j.jpowsour.2013.07.107

25. W. Pu, X. He, L. Wang, Z. Tian, C. Jiang et al., Preparation of P(AN-MMA) gel electrolyte for Li-ion batteries. Ionics **14**, 27–31 (2008). https://doi.org/10.1007/s11581-007-0155-2

26. J. Cao, L. Wang, X. He, M. Fang, J. Gao et al., In situ prepared nano-crystalline TiO_2–poly(methyl methacrylate) hybrid enhanced composite polymer electrolyte for Li-ion batteries. J. Mater. Chem. A **1**, 5955–5961 (2013). https://doi.org/10.1039/C3TA00086A

27. S. Zhang, J. Cao, Y. Shang, L. Wang, X. He et al., Nanocomposite polymer membrane derived from nano TiO_2-PMMA and glass fiber nonwoven: high thermal endurance and cycle stability in lithium ion battery applications. J. Mater. Chem. A **3**, 17697–17703 (2015). https://doi.org/10.1039/C5TA02781K

28. Y. Li, H. Shimizu, Compatibilization by homopolymer: significant improvements in the modulus and tensile strength of PPC/PMMA blends by the addition of a small amount of PVAc. ACS Appl. Mater. Interfaces **1**, 1650–1655 (2009). https://doi.org/10.1021/am900314k

29. P. Pal, A. Ghosh, Influence of TiO_2 nano-particles on charge carrier transport and cell performance of $PMMA-LiClO_4$ based nano-composite electrolytes. Electrochim. Acta **260**, 157–167 (2018). https://doi.org/10.1016/j.electacta.2017.11.070

30. Z. Tian, W. Pu, X. He, C. Wan, C. Jiang, Preparation of a microporous polymer electrolyte based on poly(vinyl chloride)/poly(acrylonitrile-butyl acrylate) blend for Li-ion batteries. Electrochim. Acta **52**, 3199–3206 (2007). https://doi.org/10.1016/j.electacta.2006.09.068

31. H. Buschmann, J. Dölle, S. Berendts, A. Kuhn, P. Bottke et al., Structure and dynamics of the fast lithium ion conductor "$Li_7La_3Zr_2O_{12}$." Phys. Chem. Chem. Phys. **13**, 19378–19392 (2011). https://doi.org/10.1039/c1cp22108f

32. J.B. Bates, N.J. Dudney, G.R. Gruzalski, R.A. Zuhr, A. Choudhury et al., Fabrication and characterization of amorphous lithium electrolyte thin films and rechargeable thin-film batteries. J. Power. Sources **43**, 103–110 (1993). https://doi.org/10.1016/0378-7753(93)80106-y

33. V. Thangadurai, W. Weppner, $Li_6ALa_2Ta_2O_{12}$ (A = Sr, Ba): novel garnet-like oxides for fast lithium ion conduction. Adv. Funct. Mater. **15**, 107–112 (2005). https://doi.org/10.1002/adfm.200400044

34. R. Kanno, M. Murayama, Lithium ionic conductor thio-LISICON: the Li_2S–GeS_2–P_2S_5 system. J. Electrochem. Soc. **148**, A742 (2001). https://doi.org/10.1149/1.1379028

35. M. Murayama, R. Kanno, M. Irie, S. Ito, T. Hata et al., Synthesis of new lithium ionic conductor thio-LISICON—lithium silicon sulfides system. J. Solid State Chem. **168**, 140–148 (2002). https://doi.org/10.1006/jssc.2002.9701

36. H. Ben youcef, O. Garcia-Calvo, N. Lago, S. Devaraj, M. Armand, Cross-linked solid polymer electrolyte for all-solid-state rechargeable lithium batteries. Electrochim. Acta **220**, 587–594 (2016). https://doi.org/10.1016/j.electacta.2016.10.122

37. L. Long, S. Wang, M. Xiao, Y. Meng, Polymer electrolytes for lithium polymer batteries. J. Mater. Chem. A **4**, 10038–10069 (2016). https://doi.org/10.1039/C6TA02621D

38. Z. Wei, Z. Zhang, S. Chen, Z. Wang, X. Yao et al., UV-cured polymer electrolyte for $LiNi_{0.85}Co_{0.05}Al_{0.1}O_2$// Li solid state battery working at ambient temperature. Energy Storage Mater. **22**, 337–345 (2019). https://doi.org/10.1016/j.ensm.2019.02.004

39. S.H. Siyal, M. Li, H. Li, J.-L. Lan, Y. Yu et al., Ultraviolet irradiated PEO/LATP composite gel polymer electrolytes for lithium-metallic batteries (LMBs). Appl. Surf. Sci. **494**, 1119–1126 (2019). https://doi.org/10.1016/j.apsusc.2019.07.179

40. C. Liu, S. Wang, X. Wu, S. Xiao, C. Liu et al., In situ construction of zwitterionic polymer electrolytes with synergistic cation–anion regulation functions for lithium metal batteries. Adv. Funct. Mater. **34**, 2307248 (2024). https://doi.org/10.1002/adfm.202307248

41. Y.M. Jeon, S. Kim, M. Lee, W.B. Lee, J.H. Park, Polymer-clay nanocomposite solid-state electrolyte with selective cation transport boosting and retarded lithium dendrite formation. Adv. Energy Mater. **10**, 2003114 (2020). https://doi.org/10.1002/aenm.202003114

42. Y. Li, X. Wang, H. Zhou, X. Xing, A. Banerjee et al., Thin solid electrolyte layers enabled by nanoscopic polymer binding. ACS Energy Lett. **5**, 955–961 (2020). https://doi.org/10.1021/acsenergylett.0c00040

43. H. Wu, B. Tang, X. Du, J. Zhang, X. Yu et al., LiDFOB initiated in situ polymerization of novel eutectic solution enables room-temperature solid lithium metal batteries. Adv. Sci. **7**, 2003370 (2020). https://doi.org/10.1002/advs.202003370

44. Y. Wang, J. Ju, S. Dong, Y. Yan, F. Jiang et al., Facile design of sulfide-based all solid-state lithium metal battery: in situ polymerization within self-supported porous argyrodite skeleton. Adv. Funct. Mater. **31**, 2101523 (2021). https://doi.org/10.1002/adfm.202101523

45. Y. Yan, J. Ju, S. Dong, Y. Wang, L. Huang et al., In situ polymerization permeated three-dimensional Li+-percolated porous oxide ceramic framework boosting all solid-state lithium metal battery. Adv. Sci. **8**, 2003887 (2021). https://doi.org/10.1002/advs.202003887

46. K. Zhang, F. Wu, X. Wang, L. Zheng, X. Yang et al., An ion-dipole-reinforced polyether electrolyte with ion-solvation cages enabling high–voltage-tolerant and ion-conductive solid-state lithium metal batteries. Adv. Funct. Mater. **32**, 2270031 (2022). https://doi.org/10.1002/adfm.202270031

47. S. Huo, L. Sheng, W. Xue, L. Wang, H. Xu et al., Challenges of stable ion pathways in cathode electrode for all-solid-state lithium batteries: a review. Adv. Energy Mater. **13**, 2204343 (2023). https://doi.org/10.1002/aenm.202204343

48. Y.Q. Mi, W. Deng, C. He, O. Eksik, Y.P. Zheng et al., In situ polymerized 1, 3-dioxolane electrolyte for integrated solid-state lithium batteries. Angew. Chem. Int. Ed. **62**, e202218621 (2023). https://doi.org/10.1002/anie.202218621

49. B. Deng, M.-X. Jing, L.-X. Li, R. Li, H. Yang et al., Nano-zirconia boosting the ionic conductivity and lithium dendrite inhibition ability of a poly(1, 3-dioxolane) solid electrolyte for high-voltage solid-state lithium batteries. Sustain. Energy Fuels **5**, 5461–5470 (2021). https://doi.org/10.1039/D1SE01132D

50. T. Chen, H. Wu, J. Wan, M. Li, Y. Zhang et al., Synthetic poly-dioxolane as universal solid electrolyte interphase for stable lithium metal anodes. J. Energy Chem. **62**, 172–178 (2021). https://doi.org/10.1016/j.jechem.2021.03.018

51. H. Huang, D. Li, L. Hou, H. Du, H. Wei et al., Advanced protective layer design on the surface of Mg-based metal and application in batteries: challenges and progress. J. Power. Sources **542**, 231755 (2022). https://doi.org/10.1016/j.jpowsour.2022.231755

52. G. Zheng, C. Wang, A. Pei, J. Lopez, F. Shi et al., High-performance lithium metal negative electrode with a soft and flowable polymer coating. ACS Energy Lett. **1**, 1247–1255 (2016). https://doi.org/10.1021/acsenergylett.6b00456

53. J. Chen, H. Lu, X. Zhang, Y. Zhang, J. Yang et al., Electrochemical polymerization of nonflammable electrolyte enabling fast-charging lithium-sulfur battery. Energy Storage Mater. **50**, 387–394 (2022). https://doi.org/10.1016/j.ensm.2022.05.044

54. N. Wang, X. Zhang, Z. Ju, X. Yu, Y. Wang et al., Thickness-independent scalable high-performance Li–S batteries with high areal sulfur loading via electron-enriched carbon framework. Nat. Commun. **12**, 4519 (2021). https://doi.org/10.1038/s41467-021-24873-4

55. X. Gao, X. Zheng, Y. Tsao, P. Zhang, X. Xiao et al., All-solid-state lithium–sulfur batteries enhanced by redox mediators. J. Am. Chem. Soc. **143**, 18188–18195 (2021). https://doi.org/10.1021/jacs.1c07754

56. G. Xu, A. Kushima, J. Yuan, H. Dou, W. Xue et al., *Ad hoc* solid electrolyte on acidized carbon nanotube paper improves cycle life of lithium–sulfur batteries. Energy Environ. Sci. **10**, 2544–2551 (2017). https://doi.org/10.1039/C7EE01898C

57. L. Ma, M.S. Kim, L.A. Archer, Stable artificial solid electrolyte interphases for lithium batteries. Chem. Mater. **29**, 4181–4189 (2017). https://doi.org/10.1021/acs.chemmater.6b03687

58. F.-Q. Liu, W.-P. Wang, Y.-X. Yin, S.-F. Zhang, J.-L. Shi et al., Upgrading traditional liquid electrolyte via in situ gelation for future lithium metal batteries. Sci. Adv. **4**, eaat5383 (2018). https://doi.org/10.1126/sciadv.aat5383

59. W.-P. Wang, J. Zhang, Y.-X. Yin, H. Duan, J. Chou et al., A rational reconfiguration of electrolyte for high-energy and long-life lithium-chalcogen batteries. Adv. Mater. **32**, e2000302 (2020). https://doi.org/10.1002/adma.202000302

60. Y. Yamashita, M. Okada, H. Kasahara, Kinetic studies on the polymerization of 1,3-dioxolane catalyzed by triethyl oxonium tetrafluoroborate. Makromol. Chem. **117**, 256–264 (1968). https://doi.org/10.1002/macp.1968.021170124

61. Y. Yamashita, M. Okada, K. Suyama, H. Kasahara, Equilibrium polymerization of 1,3-dioxolane. Makromol. Chem. **114**, 146–154 (1968). https://doi.org/10.1002/macp.1968.021140111

62. S. Sasaki, Y. Takahashi, H. Tadokoro, Structural studies of polyformals. II. Crystal structure of poly-1, 3-dioxolane: modification II. J. Polym. Sci. Polym. Phys. Ed. **10**, 2363–2378 (1972). https://doi.org/10.1002/pol.1972.180101206

63. L. Kong, H. Zhan, Y. Li, Y. Zhou, In situ fabrication of lithium polymer battery basing on a novel electro-polymerization technique. Electrochem. Commun. **9**, 2557–2563 (2007). https://doi.org/10.1016/j.elecom.2007.08.001

64. Q. Zhao, X. Liu, S. Stalin, K. Khan, L.A. Archer, Solid-state polymer electrolytes with in-built fast interfacial transport for secondary lithium batteries. Nat. Energy **4**, 365–373 (2019). https://doi.org/10.1038/s41560-019-0349-7

65. J. Zhou, T. Qian, J. Liu, M. Wang, L. Zhang et al., High-safety all-solid-state lithium-metal battery with high-ionic-conductivity thermoresponsive solid polymer electrolyte. Nano Lett. **19**, 3066–3073 (2019). https://doi.org/10.1021/acs.nanolett.9b00450

66. C.-Z. Zhao, Q. Zhao, X. Liu, J. Zheng, S. Stalin et al., Rechargeable lithium metal batteries with an In-built solid-state polymer electrolyte and a high voltage/loading Ni-rich layered cathode. Adv. Mater. **32**, e1905629 (2020). https://doi.org/10.1002/adma.201905629

67. Y. Huang, S. Liu, Q. Chen, K. Jiao, B. Ding et al., Constructing highly conductive and thermomechanical stable quasi-solid electrolytes by self-polymerization of liquid electrolytes within porous polyimide nanofiber films. Adv. Funct. Mater. **32**, 2201496 (2022). https://doi.org/10.1002/adfm.202201496

68. H. Yang, B. Zhang, M. Jing, X. Shen, L. Wang et al., In situ catalytic polymerization of a highly homogeneous PDOL composite electrolyte for long-cycle high-voltage solid-state lithium batteries. Adv. Energy Mater. **12**, 2270162 (2022). https://doi.org/10.1002/aenm.202270162

69. H. Xu, J. Zhang, H. Zhang, J. Long, L. Xu et al., In situ topological interphases boosting stable solid-state lithium metal batteries. Adv. Energy Mater. **13**, 2204411 (2023). https://doi.org/10.1002/aenm.202204411

70. P.H. Plesch, P.H. Westermann, The polymerization of 1,3-dioxolane. I. Structure of the polymer and thermodynamics of its formation. J. Polym. Sci C Polym. Symp. **16**, 3837–3843 (1967). https://doi.org/10.1002/polc.5070160724

71. D. Aurbach, O. Youngman, P. Dan, The electrochemical behavior of 1, 3-dioxolane—LiClO$_4$ solutions—II. Contaminated solutions. Electrochim. Acta **35**, 639–655 (1990). https://doi.org/10.1016/0013-4686(90)87056-8

72. H. Xu, H. Zhang, J. Ma, G. Xu, T. Dong et al., Overcoming the challenges of 5 V spinel LiNi$_{0.5}$Mn$_{1.5}$O$_4$ cathodes with solid polymer electrolytes. ACS Energy Lett. **4**, 2871–2886 (2019). https://doi.org/10.1021/acsenergylett.9b01871

73. G.H. Newman, R.W. Francis, L.H. Gaines, B.M.L. Rao, Hazard investigations of LiClO$_4$/dioxolane electrolyte. J. Electrochem. Soc. **127**, 2025–2027 (1980). https://doi.org/10.1149/1.2130056

74. Q. Liu, L. Wang, X. He, Toward practical solid-state polymer lithium batteries by in situ polymerization process: a review. Adv. Energy Mater. **13**, 2300798 (2023). https://doi.org/10.1002/aenm.202300798

75. Q. Liu, B. Cai, S. Li, Q. Yu, F. Lv et al., Long-cycling and safe lithium metal batteries enabled by the synergetic strategy of ex situ anodic pretreatment and an in-built gel polymer electrolyte. J. Mater. Chem. A **8**, 7197–7204 (2020). https://doi.org/10.1039/D0TA02148B

76. S. Wen, C. Luo, Q. Wang, Z. Wei, Y. Zeng et al., Integrated design of ultrathin crosslinked network polymer electrolytes for flexible and stable all-solid-state lithium batteries. Energy Storage Mater. **47**, 453–461 (2022). https://doi.org/10.1016/j.ensm.2022.02.035

77. H. Cheng, J. Zhu, H. Jin, C. Gao, H. Liu et al., In situ initiator-free gelation of highly concentrated lithium bis(fluorosulfonyl)imide-1, 3-dioxolane solid polymer electrolyte for high performance lithium-metal batteries. Mater. Today Energy **20**, 100623 (2021). https://doi.org/10.1016/j.mtener.2020.100623

78. J. Zheng, W. Zhang, C. Huang, Z. Shen, X. Wang et al., In-situ polymerization with dual-function electrolyte additive toward future lithium metal batteries. Mater. Today Energy **26**, 100984 (2022). https://doi.org/10.1016/j.mtener.2022.100984

79. W. Li, J. Gao, H. Tian, X. Li, S. He et al., SnF$_2$-catalyzed formation of polymerized dioxolane as solid electrolyte and its thermal decomposition behavior. Angew. Chem. Int. Ed. **61**, e202114805 (2022). https://doi.org/10.1002/anie.202114805

80. S. Zheng, Y. Chen, K. Chen, S. Yang, R. Bagherzadeh et al., In situ construction of polyether-based composite electrolyte with bi-phase ion conductivity and stable electrolyte/electrode interphase for solid-state lithium metal batteries. J. Mater. Chem. A **10**, 19641–19648 (2022). https://doi.org/10.1039/D2TA02229J

81. Z. Li, W. Tang, Y. Deng, M. Zhou, X. Wang et al., Enabling highly stable lithium metal batteries by using dual-function additive catalyzed in-built quasi-solid-state polymer electrolytes. J. Mater. Chem. A **10**, 23047–23057 (2022). https://doi.org/10.1039/D2TA06153H

82. S. Wang, L. Zhou, M.K. Tufail, L. Yang, P. Zhai et al., In-Situ synthesized Non-flammable gel polymer electrolyte enable highly safe and Dendrite-Free lithium metal batteries. Chem. Eng. J. **415**, 128846 (2021). https://doi.org/10.1016/j.cej.2021.128846

83. J. Xiang, Y. Zhang, B. Zhang, L. Yuan, X. Liu et al., A flame-retardant polymer electrolyte for high performance lithium metal batteries with an expanded operation temperature. Energy Environ. Sci. **14**, 3510–3521 (2021). https://doi.org/10.1039/D1EE00049G

84. J. Zhao, M. Li, H. Su, Y. Liu, P. Bai et al., In situ fabricated non-flammable quasi-solid electrolytes for Li-metal batteries. Small Meth. **7**, 2300228 (2023). https://doi.org/10.1002/smtd.202300228

85. J. Wei, H. Yue, Z. Shi, Z. Li, X. Li et al., In situ gel polymer electrolyte with inhibited lithium dendrite growth and enhanced interfacial stability for lithium-metal batteries. ACS Appl. Mater. Interfaces **13**, 32486–32494 (2021). https://doi.org/10.1021/acsami.1c07032

86. M. Xie, Y. Wu, Y. Liu, P.P. Yu, R. Jia et al., Pathway of in situ polymerization of 1, 3-dioxolane in LiPF6 electrolyte on Li metal anode. Mater. Today Energy 21, 100730 (2021). https://doi.org/10.1016/j.mtener.2021.100730

87. A. Hu, Z. Liao, J. Huang, Y. Zhang, Q. Yang et al., In-situ construction of dual lithium-ion migration channels in polymer electrolytes for lithium metal batteries. Chem. Eng. J. 448, 137661 (2022). https://doi.org/10.1016/j.cej.2022.137661

88. P. Cheng, H. Zhang, Q. Ma, W. Feng, H. Yu et al., Highly salt-concentrated electrolyte comprising lithium bis(fluorosulfonyl)imide and 1, 3-dioxolane-based ether solvents for 4-V-class rechargeable lithium metal cell. Electrochim. Acta 363, 137198 (2020). https://doi.org/10.1016/j.electacta.2020.137198

89. G. Yang, W. Hou, Y. Zhai, Z. Chen, C. Liu et al., Polymeric concentrated electrolyte enables simultaneous stabilization of electrode/electrolyte interphases for quasi-solid-state lithium metal batteries. EcoMat 5, e12325 (2023). https://doi.org/10.1002/eom2.12325

90. Y. Wu, J. Ma, H. Jiang, L. Wang, F. Zhang et al., Confined in situ polymerization of poly(1, 3-dioxolane) and poly(vinylene carbonate)-based quasi-solid polymer electrolyte with improved uniformity for lithium metal batteries. Mater. Today Energy 32, 101239 (2023). https://doi.org/10.1016/j.mtener.2022.101239

91. G. Yang, Y. Zhai, J. Yao, S. Song, L. Lin et al., Synthesis and properties of poly(1, 3-dioxolane) in situ quasi-solid-state electrolytes via a rare-earth triflate catalyst. Chem. Commun. 57, 7934–7937 (2021). https://doi.org/10.1039/d1cc02916a

92. L. Zhang, H. Gao, S. Xiao, J. Li, T. Ma et al., In-situ construction of ceramic–polymer all-solid-state electrolytes for high-performance room-temperature lithium metal batteries. ACS Mater. Lett. 4, 1297–1305 (2022). https://doi.org/10.1021/acsmaterialslett.2c00238

93. W. Zhang, S. Zhang, L. Fan, L. Gao, X. Kong et al., Tuning the LUMO energy of an organic interphase to stabilize lithium metal batteries. ACS Energy Lett. 4, 644–650 (2019). https://doi.org/10.1021/acsenergylett.8b02483

94. Y.-K. Han, J. Yoo, T. Yim, Distinct reaction characteristics of electrolyte additives for high-voltage lithium-ion batteries: tris(trimethylsilyl) phosphite, borate, and phosphate. Electrochim. Acta 215, 455–465 (2016). https://doi.org/10.1016/j.electacta.2016.08.131

95. Y. Liu, X. Tao, Y. Wang, C. Jiang, C. Ma et al., Self-assembled monolayers direct a LiF-rich interphase toward long-life lithium metal batteries. Science 375, 739–745 (2022). https://doi.org/10.1126/science.abn1818

96. Q. Zhao, S. Stalin, L.A. Archer, Stabilizing metal battery anodes through the design of solid electrolyte interphases. Joule 5, 1119–1142 (2021). https://doi.org/10.1016/j.joule.2021.03.024

97. P. Zhai, T. Wang, H. Jiang, J. Wan, Y. Wei et al., 3D artificial solid-electrolyte interphase for lithium metal anodes enabled by insulator-metal-insulator layered heterostructures. Adv.

98. L. Ye, X. Li, A dynamic stability design strategy for lithium metal solid state batteries. Nature 593, 218–222 (2021). https://doi.org/10.1038/s41586-021-03486-3

99. H. Xie, C. Yang, Y. Ren, S. Xu, T.R. Hamann et al., Amorphous-carbon-coated 3D solid electrolyte for an electrochemomechanically stable lithium metal anode in solid-state batteries. Nano Lett. 21, 6163–6170 (2021). https://doi.org/10.1021/acs.nanolett.1c01748

100. Y. Wang, Z. Wang, L. Zhao, Q. Fan, X. Zeng et al., Lithium metal electrode with increased air stability and robust solid electrolyte interphase realized by silane coupling agent modification. Adv. Mater. 33, e2008133 (2021). https://doi.org/10.1002/adma.202008133

101. H. Wan, Z. Wang, S. Liu, B. Zhang, X. He et al., Critical interphase overpotential as a lithium dendrite-suppression criterion for all-solid-state lithium battery design. Nat. Energy 8, 473–481 (2023). https://doi.org/10.1038/s41560-023-01231-w

102. P. Jiang, J. Cao, B. Wei, G. Qian, S. Wang et al., LiF involved interphase layer enabling thousand cycles of LAGP-based solid-state Li metal batteries with 80% capacity retention. Energy Storage Mater. 48, 145–154 (2022). https://doi.org/10.1016/j.ensm.2022.03.017

103. J. Li, H. Hu, W. Fang, J. Ding, D. Yuan et al., Impact of fluorine-based lithium salts on SEI for all-solid-state PEO-based lithium metal batteries. Adv. Funct. Mater. 33, 2303718 (2023). https://doi.org/10.1002/adfm.202303718

104. C. Guo, K. Du, R. Tao, Y. Guo, S. Yao et al., Inorganic filler enhanced formation of stable inorganic-rich solid electrolyte interphase for high performance lithium metal batteries. Adv. Funct. Mater. 33, 2301111 (2023). https://doi.org/10.1002/adfm.202301111

105. H. Sun, X. Xie, Q. Huang, Z. Wang, K. Chen et al., Fluorinated poly-oxalate electrolytes stabilizing both anode and cathode interfaces for all-solid-state Li/NMC811 batteries. Angew. Chem. Int. Ed. 60, 18335–18343 (2021). https://doi.org/10.1002/anie.202107667

106. J. Xie, S.-Y. Sun, X. Chen, L.-P. Hou, B.-Q. Li et al., Fluorinating the solid electrolyte interphase by rational molecular design for practical lithium-metal batteries. Angew. Chem. Int. Ed. 61, e202204776 (2022). https://doi.org/10.1002/anie.202204776

107. A. Hu, W. Chen, X. Du, Y. Hu, T. Lei et al., An artificial hybrid interphase for an ultrahigh-rate and practical lithium metal anode. Energy Environ. Sci. 14, 4115–4124 (2021). https://doi.org/10.1039/D1EE00508A

108. X. Pei, Y. Li, T. Ou, X. Liang, Y. Yang et al., Li-N interaction induced deep eutectic gel polymer electrolyte for high performance lithium-metal batteries. Angew. Chem. Int. Ed. 61, e202205075 (2022). https://doi.org/10.1002/anie.202205075

109. X. Yi, Y. Guo, S. Chi, S. Pan, C. Geng et al., Surface Li₂CO₃ mediated phosphorization enables compatible interfaces of composite polymer electrolyte for solid-state

lithium batteries. Adv. Funct. Mater. **33**, 2303574 (2023). https://doi.org/10.1002/adfm.202303574

110. M.-X. Jing, H. Yang, C. Han, F. Chen, L.-K. Zhang et al., Synergistic enhancement effects of LLZO fibers and interfacial modification for polymer solid electrolyte on the ambient-temperature electrochemical performances of solid-state battery. J. Electrochem. Soc. **166**, A3019–A3027 (2019). https://doi.org/10.1149/2.1171913jes

111. M.-X. Jing, H. Yang, C. Han, F. Chen, W.-Y. Yuan et al., Improving room-temperature electrochemical performance of solid-state lithium battery by using electrospun $La_2Zr_2O_7$ fibers-filled composite solid electrolyte. Ceram. Int. **45**, 18614–18622 (2019). https://doi.org/10.1016/j.ceramint.2019.06.085

112. J.Y. Kim, O.B. Chae, M. Wu, E. Lim, G. Kim et al., Extraordinary dendrite-free Li deposition on highly uniform facet wrinkled Cu substrates in carbonate electrolytes. Nano Energy **82**, 105736 (2021). https://doi.org/10.1016/j.nanoen.2020.105736

113. J. Wang, Q. Kang, J. Yuan, Q. Fu, C. Chen et al., Dendrite-free lithium and sodium metal anodes with deep plating/stripping properties for lithium and sodium batteries. Carbon Energy **3**, 153–166 (2021). https://doi.org/10.1002/cey2.94

114. J. Duan, L. Huang, T. Wang, Y. Huang, H. Fu et al., Shaping the contact between Li metal anode and solid-state electrolytes. Adv. Funct. Mater. **30**, 1908701 (2020). https://doi.org/10.1002/adfm.201908701

115. Q. Li, S. Zhu, Y. Lu, 3D porous Cu current collector/Li-metal composite anode for stable lithium-metal batteries. Adv. Funct. Mater. **27**, 1606422 (2017). https://doi.org/10.1002/adfm.201606422

116. Q. Wu, M. Fang, S. Jiao, S. Li, S. Zhang et al., Phase regulation enabling dense polymer-based composite electrolytes for solid-state lithium metal batteries. Nat. Commun. **14**, 6296 (2023). https://doi.org/10.1038/s41467-023-41808-3

117. J. Li, Y. Ji, H. Song, S. Chen, S. Ding et al., Insights into the interfacial degradation of high-voltage all-solid-state lithium batteries. Nano-Micro Lett. **14**, 191 (2022). https://doi.org/10.1007/s40820-022-00936-z

118. Y. Ma, J.H. Teo, F. Walther, Y. Ma, R. Zhang et al., Advanced nanoparticle coatings for stabilizing layered Ni-rich oxide cathodes in solid-state batteries. Adv. Funct. Mater. **32**, 2270135 (2022). https://doi.org/10.1002/adfm.202270135

119. W. Bao, G. Qian, L. Zhao, Y. Yu, L. Su et al., Simultaneous enhancement of interfacial stability and kinetics of single-crystal $LiNi_{0.6}Mn_{0.2}Co_{0.2}O_2$ through optimized surface coating and doping. Nano Lett. **20**, 8832–8840 (2020). https://doi.org/10.1021/acs.nanolett.0c03778

120. J. Zhao, J. Zhang, P. Hu, J. Ma, X. Wang et al., A sustainable and rigid-flexible coupling cellulose-supported poly(propylene carbonate) polymer electrolyte towards 5 V high voltage lithium batteries. Electrochim. Acta **188**, 23–30 (2016). https://doi.org/10.1016/j.electacta.2015.11.088

121. M. Liu, D. Zhou, Y.-B. He, Y. Fu, X. Qin et al., Novel gel polymer electrolyte for high-performance lithium–sulfur batteries. Nano Energy **22**, 278–289 (2016). https://doi.org/10.1016/j.nanoen.2016.02.008

122. L.-X. Li, R. Li, Z.-H. Huang, M.-Q. Liu, J. Xiang et al., High-performance gel electrolyte for enhanced interface compatibility and lithium metal stability in high-voltage lithium battery. Colloids Surf. A Physicochem. Eng. Aspects **651**, 129665 (2022). https://doi.org/10.1016/j.colsurfa.2022.129665

123. Y. Liu, Y. Xu, Porous membrane host-derived in situ polymer electrolytes with double-stabilized electrode interface enable long cycling lithium metal batteries. Chem. Eng. J. **433**, 134471 (2022). https://doi.org/10.1016/j.cej.2021.134471

124. Z. Geng, Y. Huang, G. Sun, R. Chen, W. Cao et al., In-situ polymerized solid-state electrolytes with stable cycling for $Li/LiCoO_2$ batteries. Nano Energy **91**, 106679 (2022). https://doi.org/10.1016/j.nanoen.2021.106679

125. J. Ma, X. Feng, Y. Wu, Y. Wang, P. Liu et al., Stable sodium anodes for sodium metal batteries (SMBs) enabled by in situ formed quasi solid-state polymer electrolyte. J. Energy Chem. **77**, 290–299 (2023). https://doi.org/10.1016/j.jechem.2022.09.040

126. S. Song, W. Gao, G. Yang, Y. Zhai, J. Yao et al., Hybrid poly-ether/carbonate ester electrolyte engineering enables high oxidative stability for quasi-solid-state lithium metal batteries. Mater. Today Energy **23**, 100893 (2022). https://doi.org/10.1016/j.mtener.2021.100893

127. K. Khan, Z. Tu, Q. Zhao, C. Zhao, L.A. Archer, Synthesis and properties of poly-ether/ethylene carbonate electrolytes with high oxidative stability. Chem. Mater. **31**, 8466–8472 (2019). https://doi.org/10.1021/acs.chemmater.9b02823

128. J. Yu, X. Lin, J. Liu, J.T.T. Yu, M.J. Robson et al., In situ fabricated quasi-solid polymer electrolyte for high-energy-density lithium metal battery capable of subzero operation. Adv. Energy Mater. **12**, 2102932 (2022). https://doi.org/10.1002/aenm.202102932

129. H. Yang, M.-X. Jing, H.-P. Li, W.-Y. Yuan, B. Deng et al., 'Environment-friendly' polymer solid electrolyte membrane via a rapid surface-initiating polymeration strategy. Chem. Eng. J. **421**, 129710 (2021). https://doi.org/10.1016/j.cej.2021.129710

130. Z.K. Liu, J. Guan, H.X. Yang, P.X. Sun, N.W. Li et al., Ternary-salt solid polymer electrolyte for high-rate and long-life lithium metal batteries. Chem. Commun. **58**, 10973–10976 (2022). https://doi.org/10.1039/D2CC04128F

131. L.-X. Li, R. Li, Z.-H. Huang, H. Yang, M.-Q. Liu et al., A multifunctional gradient solid electrolyte remarkably improving interface compatibility and ion transport in solid-state lithium battery. ACS Appl. Mater. Interfaces **14**, 30786–30795 (2022). https://doi.org/10.1021/acsami.2c05578

132. J. Ma, Y. Wu, H. Jiang, X. Yao, F. Zhang et al., In situ directional polymerization of poly(1, 3-dioxolane) solid electrolyte induced by cellulose paper-based composite separator for lithium metal batteries. Energy Environ. Mater. **6**, 12370 (2023). https://doi.org/10.1002/eem2.12370

133. X. Li, L. Cong, S. Ma, S. Shi, Y. Li et al., Low resistance and high stable solid–liquid electrolyte interphases enable

high-voltage solid-state lithium metal batteries. Adv. Funct. Mater. **31**, 2010611 (2021). https://doi.org/10.1002/adfm.202010611

134. B. Han, P. Jiang, S. Li, X. Lu, Functionalized gel polymer electrolyte membrane for high performance Li metal batteries. Solid State Ion. **361**, 115572 (2021). https://doi.org/10.1016/J.SSI.2021.115572

135. J. Sun, X. Yao, Y. Li, Q. Zhang, C. Hou et al., Composite solid electrolytes: facilitating interfacial stability via bilayer heterostructure solid electrolyte toward high-energy, safe and adaptable lithium batteries. Adv. Energy Mater. **10**, 2070131 (2020). https://doi.org/10.1002/aenm.202070131

136. Y. Liu, Y. Xu, Y. Zhang, C. Yu, X. Sun, Thin $Li_{1.3}Al_{0.3}Ti_{1.7}(PO_4)_3$-based composite solid electrolyte with a reinforced interface of in situ formed poly(1, 3-dioxolane) for lithium metal batteries. J. Colloid Interface Sci. **644**, 53–63 (2023). https://doi.org/10.1016/j.jcis.2023.03.182

137. D. Chen, M. Zhu, P. Kang, T. Zhu, H. Yuan et al., Self-enhancing gel polymer electrolyte by in situ construction for enabling safe lithium metal battery. Adv. Sci. **9**, e2103663 (2022). https://doi.org/10.1002/advs.202103663

138. Y. Li, W. Zhang, Q. Dou, K.W. Wong, K.M. Ng, $Li_7La_3Zr_2O_{12}$ ceramic nanofiber-incorporated composite polymer electrolytes for lithium metal batteries. J. Mater. Chem. A **7**, 3391–3398 (2019). https://doi.org/10.1039/C8TA11449H

139. Z. Shen, J. Zhong, J. Chen, W. Xie, K. Yang et al., SiO_2 nanofiber composite gel polymer electrolyte by in situ polymerization for stable Li metal batteries. Chin. Chemical Lett. **34**, 107370 (2023). https://doi.org/10.1016/j.cclet.2022.03.093

140. D. Lin, W. Liu, Y. Liu, H.R. Lee, P.C. Hsu et al., High ionic conductivity of composite solid polymer electrolyte via in situ synthesis of monodispersed SiO_2 nanospheres in poly(ethylene oxide). Nano Lett. **16**, 459–465 (2016). https://doi.org/10.1021/acs.nanolett.5b04117

141. Y.-Y. Lin, Y.-M. Chen, S.-S. Hou, J.-S. Jan, Y.-L. Lee et al., Diode-like gel polymer electrolytes for full-cell lithium ion batteries. J. Mater. Chem. A **5**, 17476–17481 (2017). https://doi.org/10.1039/C7TA04886F

142. L.-H. Chen, Z.-Y. Huang, S.-L. Chen, R.-A. Tong, H.-L. Wang et al., In situ polymerization of 1, 3-dioxolane infiltrating 3D garnet framework with high ionic conductivity and excellent interfacial stability for integrated solid-state Li metal battery. Rare Met. **41**, 3694–3705 (2022). https://doi.org/10.1007/s12598-022-02080-4

143. H. Huo, Y. Chen, J. Luo, X. Yang, X. Guo et al., Rational design of hierarchical "ceramic-in-polymer" and "polymer-in-ceramic" electrolytes for dendrite-free solid-state batteries. Adv. Energy Mater. **9**, 1804004 (2019). https://doi.org/10.1002/aenm.201804004

144. H. Liang, L. Wang, A. Wang, Y. Song, Y. Wu et al., Tailoring practically accessible polymer/inorganic composite electrolytes for all-solid-state lithium metal batteries: a review. Nano-Micro Lett. **15**, 42 (2023). https://doi.org/10.1007/s40820-022-00996-1

145. Z. Wan, D. Lei, W. Yang, C. Liu, K. Shi et al., All-solid-state batteries: low resistance–integrated all-solid-state battery achieved by $Li_7La_3Zr_2O_{12}$ nanowire upgrading polyethylene oxide (PEO) composite electrolyte and PEO cathode binder. Adv. Funct. Mater. **29**, 1970006 (2019). https://doi.org/10.1002/adfm.201970006

146. X. Zhang, S. Wang, C. Xue, C. Xin, Y. Lin et al., Self-suppression of lithium dendrite in all-solid-state lithium metal batteries with poly(vinylidene difluoride)-based solid electrolytes. Adv. Mater. **31**, e1806082 (2019). https://doi.org/10.1002/adma.201806082

147. Z. Zou, Y. Li, Z. Lu, D. Wang, Y. Cui et al., Mobile ions in composite solids. Chem. Rev. **120**, 4169–4221 (2020). https://doi.org/10.1021/acs.chemrev.9b00760

148. L. Han, C. Liao, X. Mu, N. Wu, Z. Xu et al., Flame-retardant ADP/PEO solid polymer electrolyte for dendrite-free and long-life lithium battery by generating Al P-rich SEI layer. Nano Lett. **21**, 4447–4453 (2021). https://doi.org/10.1021/acs.nanolett.1c01137

149. B. Xu, X. Li, C. Yang, Y. Li, N.S. Grundish et al., Interfacial chemistry enables stable cycling of all-solid-state Li metal batteries at high current densities. J. Am. Chem. Soc. **143**, 6542–6550 (2021). https://doi.org/10.1021/jacs.1c00752

150. W. Liu, D. Lin, J. Sun, G. Zhou, Y. Cui, Improved lithium ionic conductivity in composite polymer electrolytes with oxide-ion conducting nanowires. ACS Nano **10**, 11407–11413 (2016). https://doi.org/10.1021/acsnano.6b06797

151. N.W. Utomo, Y. Deng, Q. Zhao, X. Liu, L.A. Archer, Structure and evolution of quasi-solid-state hybrid electrolytes formed inside electrochemical cells. Adv. Mater. **34**, e2110333 (2022). https://doi.org/10.1002/adma.202110333

152. S. Huo, L. Sheng, W. Xue, L. Wang, H. Xu et al., Challenges of polymer electrolyte with wide electrochemical window for high energy solid-state lithium batteries. InfoMat **5**, e12394 (2023). https://doi.org/10.1002/inf2.12394

153. S. Xue, S. Yao, M. Jing, L. Zhu, X. Shen et al., Three-dimension ivy-structured MoS_2 nanoflakes-embedded nitrogen doped carbon nanofibers composite membrane as free-standing electrodes for Li/polysulfides batteries. Electrochim. Acta **299**, 549–559 (2019). https://doi.org/10.1016/j.electacta.2019.01.044

154. S. Li, S. Pang, X. Wu, X. Qian, S. Yao et al., Improve redox activity and cycling stability of the lithium–sulfur batteries via in situ formation of a sponge-like separator modification layer. Int. J. Energy Res. **44**, 4933–4943 (2020). https://doi.org/10.1002/er.5201

155. B. Deng, M.-X. Jing, R. Li, L.-X. Li, H. Yang et al., Integrating high ionic conductive PDOL solid/gel composite electrolyte for enhancement of interface combination and lithium dendrite inhibition of solid-state lithium battery. J. Colloid Interface Sci. **620**, 199–208 (2022). https://doi.org/10.1016/j.jcis.2022.04.008

156. Z. Zhuang, Y. Tang, B. Ju, F. Tu, In situ synthesis of graphitic C_3N_4–poly(1, 3-dioxolane) composite interlayers for stable lithium metal anodes. Sustain. Energy Fuels **5**, 2433–2440 (2021). https://doi.org/10.1039/D1SE00212K

157. X. Wang, X. Shen, P. Zhang, A.-J. Zhou, J.-B. Zhao, Promoted Li+ conduction in PEO-based all-solid-state electrolyte by hydroxyl-modified glass fiber fillers. Rare Met. **42**, 875–884 (2023). https://doi.org/10.1007/s12598-022-02218-4

158. P. Yao, B. Zhu, H. Zhai, X. Liao, Y. Zhu et al., PVDF/palygorskite nanowire composite electrolyte for 4 V rechargeable lithium batteries with high energy density. Nano Lett. **18**, 6113–6120 (2018). https://doi.org/10.1021/acs.nanolett.8b01421

159. J. Wu, T. Zhou, B. Zhong, Q. Wang, W. Liu et al., Designing anion-derived solid electrolyte interphase in a siloxane-based electrolyte for lithium-metal batteries. ACS Appl. Mater. Interfaces **14**, 27873–27881 (2022). https://doi.org/10.1021/acsami.2c05098

160. J. Fu, X. Ji, J. Chen, L. Chen, X. Fan et al., Lithium nitrate regulated sulfone electrolytes for lithium metal batteries. Angew. Chem. Int. Ed. **59**, 22194–22201 (2020). https://doi.org/10.1002/anie.202009575

161. F. Chen, M.-X. Jing, H. Yang, W.-Y. Yuan, M.-Q. Liu et al., Improved ionic conductivity and Li dendrite suppression of PVDF-based solid electrolyte membrane by LLZO incorporation and mechanical reinforcement. Ionics **27**, 1101–1111 (2021). https://doi.org/10.1007/s11581-020-03891-0

162. J. Li, L. Zhu, J. Zhang, M. Jing, S. Yao et al., Approaching high performancePVDF-HFPbased solid composite electrolytes withLLTOnanorods for solid-state lithium-ion batteries. Int. J. Energy Res. **45**, 7663–7674 (2021). https://doi.org/10.1002/er.6347

163. W.-W. Shao, J.-X. Li, L. Zhong, H.-F. Wu, M.-Q. Liu et al., A high ion conductive solid electrolyte film and interface stabilization strategy for solid-state Li–S battery. Colloids Surf. A Physicochem. Eng. Aspects **679**, 132593 (2023). https://doi.org/10.1016/j.colsurfa.2023.132593

164. L. Han, L. Wang, Z. Chen, Y. Kan, Y. Hu et al., Incombustible polymer electrolyte boosting safety of solid-state lithium batteries: a review. Adv. Funct. Mater. **33**, 2300892 (2023). https://doi.org/10.1002/adfm.202300892

165. C.-B. Jin, N. Yao, Y. Xiao, J. Xie, Z. Li et al., Taming solvent–solute interaction accelerates interfacial kinetics in low-temperature lithium-metal batteries. Adv. Mater. **35**, 2208340 (2023). https://doi.org/10.1002/adma.202208340

166. J. Zhou, H. Ji, Y. Qian, J. Liu, T. Yan et al., Molecular simulations guided polymer electrolyte towards superior low-temperature solid lithium-metal batteries. ACS Appl. Mater. Interfaces **13**, 48810–48817 (2021). https://doi.org/10.1021/acsami.1c14825

167. L.E. Camacho-Forero, P.B. Balbuena, Effects of charged interfaces on electrolyte decomposition at the lithium metal anode. J. Power. Sources **472**, 228449 (2020). https://doi.org/10.1016/j.jpowsour.2020.228449

168. F. Liu, T. Li, Y. Yang, J. Yan, N. Li et al., Investigation on the copolymer electrolyte of poly(1, 3-dioxolane-co-formaldehyde). Macromol. Rapid Commun. **41**, e2000047 (2020). https://doi.org/10.1002/marc.202000047

169. Y. Du, L. Zhao, C. Xiong, Z. Sun, S. Liu et al., Ameliorating structural and electrochemical properties of traditional polydioxolane electrolytes via integrated design of ultra-stable network for solid-state batteries. Energy Storage Mater. **56**, 310–318 (2023). https://doi.org/10.1016/j.ensm.2023.01.017

170. J. Cui, Y. Du, L. Zhao, X. Li, Z. Sun et al., Thermal stable poly-dioxolane based electrolytes via a robust crosslinked network for dendrite-free solid-state li-metal batteries. Chem. Eng. J. **461**, 141973 (2023). https://doi.org/10.1016/j.cej.2023.141973

171. D.F. Miranda, C. Versek, M.T. Tuominen, T.P. Russell, J.J. Watkins, Cross-linked Block copolymer/ionic liquid self-assembled blends for polymer gel electrolytes with high ionic conductivity and mechanical strength. Macromolecules **46**, 9313–9323 (2013). https://doi.org/10.1021/ma401302r

172. S. Chen, B. Chen, J. Fan, J. Feng, Exploring the application of sustainable poly(propylene carbonate) copolymer in toughening epoxy thermosets. ACS Sustain. Chem. Eng. **3**, 2077–2083 (2015). https://doi.org/10.1021/acssuschemeng.5b00343

173. J. Qin, W. Luo, M. Li, P. Chen, S. Wang et al., A novel multi-block copolymer of CO_2-based PPC-*mb*-PBS: from simulation to experiment. ACS Sustain. Chem. Eng. **5**, 5922–5930 (2017). https://doi.org/10.1021/acssuschemeng.7b00634

174. J.H. Han, J.Y. Lee, D.H. Suh, Y.T. Hong, T.-H. Kim, Electrode-impregnable and cross-linkable poly(ethylene oxide)–poly(propylene oxide)–poly(ethylene oxide) triblock polymer electrolytes with high ionic conductivity and a large voltage window for flexible solid-state supercapacitors. ACS Appl. Mater. Interfaces **9**, 33913–33924 (2017). https://doi.org/10.1021/acsami.7b09909